CR-115742

The Human, Primate and Rabbit Ultraviolet Action Spectra

(NASA-CR-115742) THE HUMAN, PRIMATE AND RABBIT ULTRAVIOLET ACTION SPECTRA D.G. Pitts, et al (Houston Univ.) 31 Mar. 1972 59 p

CSCL 06C

N72-28063

G3/04 37588

Unclas

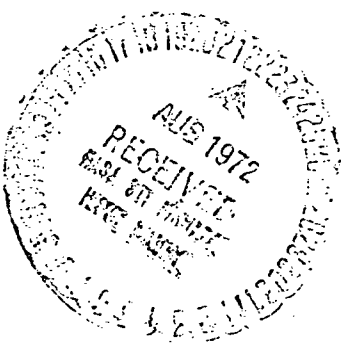

Donald Graves Pitts, O.D., Ph.D.
William Donald Gibbons, O.D., M.S.

THE HUMAN, PRIMATE AND RABBIT ULTRAVIOLET ACTION SPECTRA

Donald Graves Pitts, O.D., Ph.D.

William Donald Gibbons, O.D., M.S.

University of Houston

College of Optometry

Houston, Texas 77004

March 31, 1972

FOREWORD

The research for this report was funded by the National Aeronautics and Space Administration, Manned Space Center, under NASA contract NAS9-10836. The report was prepared by Donald G. Pitts, O.D., Ph.D., principal investigator, and William D. Gibbons, O.D., M.S., research assistant. Ophthalmology Associates, Pasadena, Texas, served as medical consultants for the human exposures. The research was accomplished between June 20, 1970 and January 31, 1972. The paper was submitted for publication on March 31, 1971.

This research is dedicated to the human volunteer subjects who showed a confidence in the research protocol above that ordinarily expected. Sincere appreciation is extended to Dr. Roger Fitch, NASA, MSC, Neurophysiology Branch for his support and contributions to the effort.

ABSTRACT

A 5000 watt xenon-mercury high pressure lamp was used to produce a continuous ultraviolet spectrum. Human and animal exposures were made to establish the photokeratitis threshold and abiotic action spectrum. The lower limit of the abiotic action spectrum was 220 nm while the upper limit was 310 nm. The radiant exposure threshold at 270 nm was 0.5×10^{-2} watts cm^{-2} for the rabbit, 0.4×10^{-2} watts cm^{-2} for the primate, and 0.4×10^{-2} watts cm^{-2} for the human. The rabbit curve was bi-peaked with minimums at 220 nm, 240 nm and 270 nm. The primate curve was tri-peaked with minimums at 220 nm, 240 nm and 270 nm. The human data showed a rather shallow curve with a minimum at 270 nm.

Formulas and calculations are given to predict minimum exposure times for ocular damage to man in outer space, to establish valid safety criteria, and to establish protective design criteria.

TABLE OF CONTENTS

	Page
Introduction	1
Instrumentation and calibration	5
Experimental procedure	9
Results	13
Discussion	15
References	28
Tables	31
Figures	38

THE HUMAN, PRIMATE AND RABBIT ULTRAVIOLET ACTION SPECTRA

I. INTRODUCTION

Purpose of the study

The objectives of this research effort were (1) to provide calibration, monitoring, and spectral analysis of the high intensity ultraviolet source; (2) to establish threshold data for photokeratitis in the rabbit, primate, and man; (3) to relate threshold data to the solar ultraviolet profile in space; (4) to predict minimum exposure times for ocular damage to man in outer space; and (5) to establish valid safety and protective design criteria.

The study was designed to establish thresholds with rabbits and primates prior to research with humans. The human data would provide a direct comparison with animal data and permit valid protective criteria to be developed. The clinical approach was rather straightforward and involved the study of the effects of ultraviolet on the corneal epithelium by the biomicroscope.

Historical review

The abiotic effect of the near (300 to 400 nm) and far (200 to 300 nm) ultraviolet light (UV) on living tissue has been known since very early times because Xenophonon mentions "snowblindness" in his treatise, Anabasis. Coordinated studies of the deleterious effects of ultraviolet light were begun in the 19th century, but were concentrated on the effects of the electric light on the eye.

The ultraviolet is not detected by the visual receptors of mammals --including man. Therefore, exposure to ultraviolet could result in ocular damage before the recipient was aware of the potential danger. Numerous cases of abiotic UV exposure resulting in keratitis of the cornea and cataracts of the lens have been reported (1,2). The UV levels involved were associated with welding arcs, high pressure pulsed lamps, and reflection of solar radiation from natural terrain (snow, desert, and water).

An extensive historical review of the literature will not be accomplished because Verhoeff et al. (3) and Buchanan et al. (4) have established extensive references and an annotated bibliography. Only a few vital references are needed to acquaint the reader with the effects of ultraviolet on the eye.

Verhoeff et al. (3) are an excellent starting point because all research data are included so that one may form his own opinions. In addition, they formulated some of the basic postulates relating ocular damage to ultraviolet and established 2.0×10^6 ergs/cm^2 as the threshold for the whole UV spectrum. Duke-Elder (2) provides an excellent summary of the research which covers threshold data, destructive and reparative processes. Bushke et al. (5) emphasize the destructive effects of UV on the corneal epithelial cell nuclei, loss of epithelial adhesion to Bowman's membrane, and the inhibiting effects of ultraviolet to the healing process.

Cogan and Kinsey (6) provide the most reliable quantified threshold data. They used a high-pressure mercury quartz lamp as a source and were limited in spectral waveband output by a prism monochromator.

Their description of the grading of ocular reaction to ultraviolet and their criteria were used extensively during this research. They established the long wavelength limit between 306-326 nm and a threshold of 0.15×10^6 ergs/cm^2 at 288 nm for the rabbit.

A central question to UV effects on corneal tissue lies in the absorption or transmission of the ultraviolet. A comparison of Kinsey (7) and Bachem's (8) corneal ultraviolet absorption curves shows that little ultraviolet below 310 nm is transmitted through the cornea and that most absorption below 310 nm occurs in the epithelium. The two sets of whole cornea absorption compare quite favorably.

The ordinary clinical photokeratitis follows a characteristic course. After exposure, there is a period of latency varying somewhat inversely with the severity of the exposure. The latency may be as short as 30 minutes and as long as 24 hours but is typically 6 to 12 hours. Conjunctivitis sets in and is accompanied with an erythema of the skin surrounding the eyelids. There is a sensation of a foreign body or "sand" in the eyes, varying degrees of photophobia, lacrimation and blepharospasm. These acute symptoms usually last from 6 to 24 hours, but almost all discomfort disappears within 48 hours. Very rarely does exposure result in permanent damage. However, the importance of the symptoms lies in the fact that the individual is incapacitated visually for varying periods of time and that the ocular system does not develop tolerance to repeated ultraviolet exposure like the skin.

The UV reaching the earth's surface provides little hazard to man under normal activities because of the filtering action of various

components of the earth's atmosphere. Absorption in the region below 85 nm is due chiefly to O_2, O, N_2 and N; between 85 and 200 nm, it is due to molecular oxygen; while from 200 to 300 nm absorption is due to ozone (9). Thus, practically all of the UV radiation shorter than 295 nm is absorbed by the earth's atmosphere.

As man seeks to expand his environment to outer space and other planets, a new situation develops in which man is constantly subject to high levels of ultraviolet radiation. Approximately two percent of the sun's total energy in space is concentrated in the abiotic UV portion of the spectrum, and there are relatively large fluctuations in intensity in the far ultraviolet due to solar flares. In space, man is not afforded the protective ultraviolet absorbing atmosphere.

If man is to accomplish his space mission objectives, he must not be incapacitated by abiotic UV radiation. Reliable and accurate tolerance limits of UV radiation are a necessity. These limits can be determined by accurately calibrating and monitoring the light energy used to produce exposures in the laboratory and by carefully and systematically relating the exposure to any resulting injury.

II. INSTRUMENTATION AND CALIBRATION

The source for the ultraviolet energy was a 5000 watt xenon-mercury high pressure lamp. It was powered by a 10 KW, DC power supply which was regulated to $\pm$0.5% and capable of delivering from 0 to 80 amperes at 25 to 50 volts to the arc electrodes. A diagram of the exposure apparatus is shown in Figure 1. The lamp housing was cooled by two blowers. Adequate cooling was available except when the lamp was operated at high amperages.

The desired waveband of ultraviolet was obtained with a model 2501 MacPherson grating monochromator. The grating was blazed for 300 nm and provided a 73% efficiency at 270 nm. The grating was grooved with 300 lines per millimeter which allowed adequate band-pass characteristics. Entrance and exit slits were set to pass a nominal full-band width of 9.9 nm. Full band pass did not exceed 10 nm for all wavebands used in these experiments; therefore, all wavebands are reported as 10 nm.

Exposure times were controlled with a Uniblitz Model 300 electronic shutter. The controls of the shutter allowed millisecond accuracy from zero to 9.9 seconds. Extented times could be obtained by adding external resistance. The electronic shutter system was calibrated using an SGD-100 photodiode and photographing the shutter response displayed on an oscilloscope. Figure 2 illustrates the shutter response time plotted against real time. Exposure times above 25 seconds were measured by a stop watch. Table I demonstrates that only six of the exposures were above the 25 second time period.

Radiant energy from the source S (Fig. 1) was brought to a focus at the monochromator entrance slit by quartz lenses L_1 and L_2. A 15 cm quartz enclosed water chamber was placed between the focusing lenses and the monochromator to remove infrared energy. The beam size at the cornea for the monochromator produced ultraviolet wavebands was 1.6 x 1.8 cm.

All previous research on the effects of ultraviolet have used subjective biomicroscopic measures as the end-point. An objective measure which lends itself to quantification was highly desirable. Since ultraviolet affects primarily the epithelial layers of the cornea, the scatter of corneal light offered promise as an objective technic.

The apparatus for measuring corneal light scatter consisted of a Zeiss biomicroscope, a scanning micrometer eyepiece modified to fit the Zeiss biomicroscope, a photomultiplier and a storage oscilloscope (Figure 3). Corneal light scatter measurements were obtained by using the slit lamp beam to section the cornea and focusing this corneal section into the scanning eyepiece mounted on the slit lamp. A 50μ fiber optic in the scanning micrometer eyepiece was then passed across the focused section of the cornea. The angle between the slit lamp light source and the eyepiece with the scanning 50μ fiber optic was fixed at 45°. The slit lamp beam sectioned the cornea normal to the cornea. Replication was assurred by aligning the first and third Purkinje images. Light received by the scanning fiber optic was passed on to the photomultiplier, amplified and displayed on the storage oscilloscope. The oscilloscope display was measured

and photographed for later analysis. The amplitude of the scatter trace on the film was measured from a microfilm reader which provided 5x magnification. A typical corneal scatter trace is shown in Figure 4. Pre-exposure measurements were used as a baseline and the change in scatter measurements were expressed as a percentage of the pre-exposure level.

Source Calibration

An Eppley 16 junction thermopile was used to calibrate the ultraviolet source (10, 11, 12). The thermopile was calibrated against an NBS standard lamp for the visible and infrared portions of the electromagneticspectrum with a ± 2 accuracy. The readout instrument was a Keithley model 150B microvolt-ammeter which was accurate to $\pm 0.5\%$. The thermopile was placed in the same position that the subject's cornea would occupy and the output of the thermopile was read from the microvolt meter.

The irradiance incident on the thermopile was determined by the following relationships:

(1) $E_e = kV_e$

E_e = irradiance (watts cm^{-2} sec^{-1})

k = calibration constant of the thermopile (5.565×10^{-3} watts cm^{-2} sec^{-1} mV)

V_e = thermopile voltage in mV

Equation (1) is valid for measurements made on light sources which have diameters at the measuring plane of the thermopile equal to the detector's surface diameter. Figure 5 provides a calibration curve of the source spectral irradiance, $E_{e(\lambda)}$, in watts cm^{-2} sec^{-1} nm.

The radiant exposure Q (watts cm^{-2}) was calculated using the following:

(2) $Q = E_e T$

Q = radiant exposure (watts cm^{-2})

E_e = irradiance (watts cm^{-2} sec^{-1})

T = exposure duration (sec)

For a given irradiance E_e, the exposure duration T could be varied to obtain different values for the radiant exposure Q.

The exposure duration T, ultraviolet irradiance E_e and radiant exposure Q were determined for each subject prior to exposure using the above calibration technics. The overall calibration accuracy was estimated to be less than $\pm$10%.

III. EXPERIMENTAL PROCEDURE

Previous data (13, 14) was used to establish the guidelines for human research. Exposures were to be made at 30%, 40% and 50% of the primate data; however, it was found that threshold had not been attained at some wavebands at these levels. Care had to be exercised since animal data had shown that a 10% irradiance increase changed a below threshold response to an above threshold response. For the human subject such a change could result in severe discomfort and pain. Thus, as the 50% primate threshold value was reached only one subject was exposed at higher values for that waveband during an experimental session. The remainder of the subjects were exposed at another waveband.

Four or five subjects were exposed at each experimental session. Prior to exposure corneal light scatter baseline data, visual acuity and a biomicroscopic examination was made on each subject. The source was calibrated, radiant exposure values determined, and exposure time calculated. The cornea of the subject's eye was placed in the center of and normal to the UV beam. Alignment of the subject was maintained by use of a head-chin rest. The subject was requested to refrain from blinking during exposure and any blinks or other movements were recorded. The corneas were exposed at 10 nm waveband steps from 220 to 310 nm. Source calibration and exposure usually took an hour for each experimental session.

Waveband exposures below 220 nm were not possible because the source energy was insufficient to make exposure time practical. The

transmission of wavelengths above 310 nm through the cornea to the lens increases rapidly. The effects of ultraviolet on the anterior epithelium of the crystalline lens is not known; therefore, exposures above 310 nm were not made. This was a safety precaution since the lens anterior epithelium must serve the human throughout life.

After exposure the subjects were examined with the biomicroscope, corneal light scatter measurements were made, and visual acuity was taken on a B&L orthorater at hourly intervals for 9 hours. Each subject was asked to describe verbally any symptoms which he had experienced.

To obtain scatter measurements, the beam from the slit lamp source was focused on the cornea and adjusted so that the beam incidence was normal to the cornea. Normal incidence was accomplished by aligning the light beam on the iris and lens in a continuous line and with a fiducial mark on the slit beam housing. The scanning fiber optic was set at a reading of 3.0 and the slit lamp adjusted so that the fiber optic probe was positioned on the posterior surface of the corneal section focused in the eyepiece. The slit lamp magnification was set at 16x. Alignment was rechecked and scatter measurements taken. Precise fixation was required for subjects undergoing scatter measurements. The slit source was checked prior to each experimental session to insure that light values did not affect the measurement. Three corneal light scatter measurements were obtained from each subject hourly during an experimental session.

Seven criteria were used to determine threshold: epithelial debris, epithelial haze, epithelial granules, photophobia, symptomatology, and corneal light scatter. Epithelial debris may be described

as small glistening bodies located in the corneal tear layer. Epithelial haze was an irregular, crackled appearance of the corneal anterior surface and was classified as an above threshold exposure. Epithelial granules were small, white, discrete, round spots located deep in the epithelial layer of the cornea. If 50 to 200 granules were seen, the exposure was threshold; above 200 granules was suprathreshold; below 50 granules was subthreshold. Photophobia was an avoidance response or verbal response that the slit lamp light bothered the subject as the cornea was examined. Symptoms and corneal light scatter were recorded to determine if they could be correlated with the ultraviolet exposure levels. This would place greater confidence in the threshold data.

Two observers independently determined the criteria status and classification of each eye. The severity of the exposure for each criterion was indicated as negative (-), probably positive but not certain ($\pm$), positive (+), moderately positive (++) and severely positive (+++). When any five of the seven criteria were positive (+), the eye was classified as above threshold (+). Three to four positive criteria were classified as probably positive, not certain ($\pm$). Fewer than three positive criteria resulted in a below threshold classification (-). The lowest radiant exposure which resulted in an above threshold classification terminated the experiment for that waveband.

All subjects were volunteer and paid $20.00 for each experimental session. The subject sample was composed of college age students. In spite of the subjects being paid, it was difficult to obtain an adequate number of subjects because of the apprehension that permanent

damage to the eye might result. Each subject was thoroughly briefed prior to the experiment and assured that no permanent damage could result.

Conventional statistical rounding procedures were used. All data was rounded to two significant figures. An experimental session covered approximately 14 hours.

IV. RESULTS

Ultraviolet exposure was made to 39 human eyes during these experiments. In prior reports (13, 14), data for 238 rabbit eyes and 83 primate eyes were presented. The raw laboratory data for biomicroscopically determined human photokeratitis thresholds (Q_{CH}) for the wavebands from 220 to 310 nm, in 10 nm steps, are presented in Table I. Each subject's response to the seven criteria and subsequent classification for wavebands from 220 to 310 nm are given in Table II. A summary of biomicroscopic determined rabbit, primate and human threhsolds in both ergs $cm^{-2} \times 10^{6}$ and watts $cm^{-2} \times 10^{-2}$ and the relative efficiency of each are listed in Table III. Relative efficiency was calculated by normalizing the threshold data to the waveband most effective in producing photokeratitis, i.e., waveband 270 nm. Figure 6 compares the biomicroscopic ultraviolet abiotic action spectrum curves for the human, primate and rabbit with the abscissa presenting the threshold exposure Q_C in watts $cm^{-2} \times 10^{-2}$ and the ordinate the waveband in nanometers.

Corneal light scatter data was analyzed in the following manner. Three meaned pre-exposure light scatter values were taken as the baseline. The amplitude of individual post-exposure light scatter responses were measured from oscilloscope photographs. A minimum of three such measures were meaned for each post-exposure examination. The means were converted into percent difference from the baseline light scatter measure. An increase in corneal light scatter above the baseline was taken as a + value. A decrease in corneal light

scatter below the baseline was taken as a - value. The data were graphed with percent change in light scatter as the ordinate and the time in hours after exposure as the abscissa. Each corneal light scatter figure presents the data for each subject and the radiant exposure in watts $cm^{-2} \times 10^{-2}$ for the particular waveband used in the exposure. Corneal light scatter results are shown in Figures 8 through 15. It should be noted that wavebands 240 nm and 280 nm did not have sufficient scatter data taken to be included in the report. Subject JBR at 300 nm was unable to maintain adequate fixation for corneal scatter measurements to be interpreted.

V. DISCUSSION

The data in Figure 6 establishes the ultraviolet abiotic action spectrum for the rabbit and primate from 220 to 310 nm. The rabbit radiant exposure threshold at 270 nm was 0.5×10^{-2} watts cm^{-2}. The threshold radiant exposure for the primate at 270 nm was 0.4×10^{-2} watts cm^{-2}. The rabbit curve presented a bi-peaked curve with minimums at 230 nm and 270 nm. The primate curve is tri-peaked with minimums at 220, 240 and 270 nm. Both the rabbit and primate curves show rapid increases in thresholds above 220 nm and above 310 nm (Table III).

The ultraviolet abiotic action spectrum for the human is not as easily defined as for the rabbit and the primate. At 260 nm and above the human threshold curve is not materially different from the primate; however, below 250 nm the human threshold curve shows radiant exposure values considerably below the data of either animal. Rather than showing peaks or minimums the human curve tends to be a rather shallow curve which gives a minimum at 270 nm of 0.4×10^{-2} watts cm^{-2}. The data indicates that the upper waveband for the ultraviolet action spectrum could be 310 nm. Likewise the data indicates that the lower waveband would be 220 nm even though ultraviolet energy was insufficient for exposures below 220 nm. Therefore, it is felt that the human ultraviolet action spectrum range is from 220 nm to 310 nm.

The experiments were not designed to produce discomfort in human subjects. One might question just how well the established thresholds for humans predicts discomfort (Table III). The exposures made at

waveband 250 nm provide an excellent insight to answer such a question. Thresholds were established at wavebands 270 nm, 280 nm, 290 nm and 260 nm prior to making exposures at 250 nm. In each of these wavebands it was found that the threshold was 80% to 100% of the primate threshold. In an attempt to prevent repetitious exposures which provided little information, it was decided to expose subjects for 250 nm at the 50% and 60% primate level. The 60% exposure for BBR provided a +++ classification response with severe discomfort, photophobia and a decrease of visual acuity from 20/20 to 20/40. The 50% exposure for APR resulted in acuity decrease to 20/30, photophobia, and moderate discomfort. The 40% exposure to PCL resulted in the decrease of visual acuity to 20/30, slight photophobia and mild discomfort. The discomfort and acuity decreases by DML at 280 nm were slightly more severe than for subject BBR at 250 nm. All human exposures at 250 nm produced discomfort at a much lower percent of the radiant exposure level than found at wavebands above 250 nm. These findings provided an excellent experience, although totally unplanned, and gave an indication of the energy levels above threshold which would result in discomfort and incapacitation. Figure 7 gives the threshold curve and a second curve 20% above threshold. Exposure to ultraviolet at an energy level below or equal to the threshold curve should result in little decrease in acuity, little or no discomfort and little impairment of visual performance. Exposures at or above the $\pm$20% curve should result in decrease of visual acuity up to 2 Snellen lines for at least 24 hours, moderate symptoms and decrease of visual performance. Photophobia should be severe enough to prevent the subject

from keeping his eyes open.

Corneal scatter measurements provide a second method of establishing ultraviolet radiant exposure thresholds. The major percentage of scatter in the cornea is caused by the epithelium. Ultraviolet in the waveband range used in this experiment is almost totally absorbed in the corneal epithelium (7, 8). Therefore, one would expect damage of the corneal epithelium to be directly related to the level of energy used in the exposure of the cornea.

Figure 13 A-D provides an example of corneal scatter data which can be explained in terms of level of the ultraviolet radiant exposure. Figure 13 D illustrates the response obtained with a low exposure level. The surface corneal epithelial cells absorb the ultraviolet and provide a scatter above and below the baseline as they die and are sloughed into the tear layer. As the energy is increased (Figure 13 C) the surface cells clear and the cornea shows a period of time in which scatter is decreased. Further increases in ultraviolet radiant exposure results in damage to deeper epithelial cells and a prolonged increase in scatter which clears very late in the experiment (Figure 13 B). Finally, the radiant exposure level is sufficient to result in corneal haze and corneal edema. This is reflected in scatter measurements which remain elevated throughout the period of the experiment and for a 24 hour post-exposure period (Figure 13 A). A further increase in radiant exposure results in sloughing of the deep epithelial cells and a clearing of the cornea as illustrated in Figure 10 B. This type of response was always accompanied with discomfort, photophobia and a decrease in visual acuity. Therefore, a corneal

light scatter response such as Figure 13 A was taken as a threshold response.

Utilizing the corneal light scatter response criteria for the determination of a threshold exposure provided the following thresholds: λ220 nm, 0.1×10^{-2} watts cm^{-2}; λ230 nm, 0.1×10^{-2} watts cm^{-2}; λ250 nm, 0.8×10^{-2} watts cm^{-2}; λ260 nm, between 0.65 and 0.74×10^{-2} watts cm^{-2}; λ270 nm, between 0.35 and 0.40×10^{-2} watts cm^{-2}; λ290 nm, 0.7×10^{-2} watts cm^{-2}; λ300 nm, 0.7×10^{-2} watts cm^{-2}; and λ310 nm, between 1.2 and 1.4×10^{-2} watts cm^{-2}. It can be seen that the corneal scatter data and biomicroscopic data compare favorably in establishing the radiant exposure threshold. An advantage of the corneal scatter method is that the response is quantified and does not rely on subjective interpretation.

Epithelial debris proved to be one criteria which was of little value in determining exposure threshold. Debris was obtained for every subject regardless of the total radiant exposure. In spite of this, debris was valuable in comparing biomicroscopic and corneal light measurements. One could predict early scatter responses by observing the debris. Later corneal scatter responses were due to a combination of debris, haze and granules. Debris was noted sooner and was greater in amount at wavelengths below 260 nm. It was less apparent and less in amount at the longer wavelengths. In above threshold measurements, debris appeared and could be determined by scatter technics but showed cyclic changes (Figure 10 A) or a clearer cornea than pre-exposure (Figure 10 B). Finally, two different types of debris were noted. There was a coarse debris which was assumed to be

related to the surface epithelial cells and a very fine debris which was related to the deeper corneal epithelial layers. The coarse debris usually occurred early post-exposure and the fine debris late after exposure. The fine debris became more noticeable after higher radiant exposures while the coarse debris was more apparent at lower radiant exposures.

Epithelial haze was not found until the radiant exposure levels approached the threshold level. It usually occurred 6 to 7 hours after exposure. Therefore, haze appears to be one of the criteria which becomes manifest as threshold is approached. Granules, like epithelial haze, did not appear until the radiant exposure level approached threshold. The size of the granules appeared directly related to wavelength. Wavelengths below 250 nm showed fine, discrete granules while wavelengths above 250 nm gave larger more coalescing type granules. Both epithelial haze and granules should contribute to increased scatter; therefore, corneal light scatter measurements should provide an excellent method of determining a threshold classification.

Photophobia provided little assistance in establishing threshold exposure levels. Photophobia did not occur for all subjects classified as threshold. Photophobia did not occur prior to 6 hours post-exposure and delayed as long as 12 hours. Photophobia was so variable between exposure levels and subjects that it was an unreliable criteria in determining threshold.

The visual acuity of all subjects classified as threshold was affected. In Table II, subjects classified as threshold and marked (-) reported hazy vision; ($\pm$) subjects had an acuity decrement of one

Snellen line and (+) subjects had an acuity decrement of two lines. Visual acuity decrement occurred within 2 hours but as long as 7 hours for some subjects. The average lapsed post-exposure time for acuity decrement was 5 hours. All subjects classified with a (+) for visual acuity showed decreases in acuity 24 hours after exposure. It was interesting to note that some subjects reported improved visual acuity with sub-threshold exposures. The improved acuity corresponded to biomicroscopic reported clearing of epithelial debris and improved or less corneal light scatter measurements. It can be concluded that ultraviolet exposure at threshold levels can result in the decrement of acuity of two Snellen lines which will begin in about 5 hours and continue for period of 24 hours.

Many subjects reported bizarre symptoms which were not related to the UV exposure. The most common related symptoms which were reported included tearing and a foreign body sensation. Only three subjects (APR, BBR and DML) reported symptoms which were considered severe enough to interfere with normal duties. Thus, if visual acuity decrements allowed performance of duties requiring vision, most of the subjects could have continued their duties.

The subjects' reactions to 220 and 230 nm exposure selected as threshold requires some discussion. Subject ACR was exposed to 220 nm with a radiant exposure Q of 0.1×10^{-2} watts cm^{-2}. The irradiance was 3.9×10^{-5} watts cm^{-2} sec^{-1} for a duration of 256 seconds. The subject blinked 39 times during exposure. The eye was injected immediately after exposure and the subject stated that the eye was uncomfortable. Within one hour, there was coarse and fine debris, the eye

was still injected and had a foreign body sensation. After two hours exposure, the eye was injected, there was tearing, foreign body sensation, slight edema of the lid margins, and severe fine and some coarse debris. The signs were the same at 4 hours after exposure but the subject reported that his VA appeared a little clearer than originally. The examination at 4 hours after exposure showed deep granules, slight fine debris, moderate large debris and a decrease in visual acuity. The eye had begun to feel more comfortable. By 6 hours post-exposure, all injections had disappeared and the subject was comfortable in spite of debris, epithelial haze and granules. This was considered a rather quick, severe reaction to the exposure and further increases in the level of radiant exposure were not warranted.

Subject RHL was exposed to 230 nm with a radiant exposure of 1.3×10^{-2} watts cm^{-2}. The irradiance was 2.8×10^{-5} watts cm^{-2} sec^{-1} for a duration of 45.5 seconds. He stated that his eye was stinging and burning during exposure. The stinging and burning sensation continued through 4 hours post-exposure. He showed a slight increase in fine and coarse debris after one hour which increased to moderate at 2 hours post-exposure. Visual acuity decreased one Snellen line at 2 hours with coarse and fine debris, epithelial haze, and granules being apparent at 3 hours post-exposure. Visual acuity returned to normal at 6 hours post-exposure but all other signs remained throughout the experimental session.

From the above observations, it was felt that the reaction of the cornea to wavebands below 250 nm was different from those found with exposures above 250 nm. The signs and symptoms occurred much earlier

post-exposure for exposures below 250 nm and subjective symptoms always returned to normal prior to completion of the experiment. For exposures above 250 nm, the symptoms did not occur until late in the experiment. Subjects exposed above threshold (PCL, APR, BBR and DML) gave maximum symptoms at 9 to 11 hours post-exposure. Visual acuity decreased quickly and returned to normal within 6 hours for exposures below 250 nm. Reduced acuity was not found on exposures above 250 nm until about 6 hours post-exposure and remained below normal for the 24 hour post-exposure examination.

It is felt that these differences were due to the difference in absorption of the different wavebands. The lower wavebands were absorbed in the outer corneal epithelial layers and manifested a rapid change. The higher wavebands were absorbed in the deeper epithelial layers and showed delayed changes because these cells are more viable. Thus, shorter wavelengths provide a rapid recoverable response while the longer wavelengths show a delayed more serious response.

In the previous reports, a method for computing minimal exposure time (T) in space to produce photokeratitis was derived from the primate and rabbit data. These data are modified in the following paragraphs so that safe exposure times may be predicted for humans.

The data required to calculate ultraviolet (UV) safe exposure criteria include solar spectral irradiance, moon spectral irradiance, transmittance of the optical media before the eyes, and the relative efficiency of UV to produce photokeratitis. The threshold data for primate corneal damage Q_{CP} are shown in Figure 6 and listed in Table IV, column 7 in watts cm^{-2} nm^{-1} x 10^{-7}. The radiant exposure threshold

data Q_{CP} are used to calculate the relative efficiency W_λ of UV by normalizing the data to the waveband (270 nm) requiring the least irradiance to produce photokeratitis. The relative efficiency W_λ for primates is shown in Table IV, column 8. The calibration procedures used in the experiments to determine the radiant exposure threshold data was estimated to be accurate to $\pm$10%. The same data are shown for human in Figure 6 and Table V. Solar spectral irradiance is given in Tables IV and V, column 2 while the moon spectral irradiance is shown in column 5 (15-21).

Several modifications to the energy take place before safe exposure times can be calculated. The moon radiant energy is modified by reflectance from the moon's surface and transmission through the spacecraft window or other optical transparencies prior to striking the cornea of the eye. Solar radiant energy is modified by transmission through the spacecraft window or other optical transparencies prior to striking the cornea. The formulas given in the following examples can be used to calculate safe exposure times for any optical transparency as long as its transmission is known. Figure 16 shows the transmission of UV through a quartz spacecraft window used for ultraviolet photography on APOLLO 15 and 16 (20). All windows associated with the other APOLLO missions and all other windows on APOLLO 15 and 16 were essentially opaque to the ultraviolet. The spectral reflectance of solar ultraviolet from the moon's surface given in Figure 17 is variable but does not exceed 3% (21). It is estimated that 3% is the worst case and constitutes an unknown safety factor in the calculations.

The solar radiation inside the spacecraft is found by multiplying the solar irradiance at each waveband by the spectral transmission of the optical transparencies placed in front of the eyes:

$$E_{\lambda ST} = E_{\lambda S} \cdot T_{\lambda}$$

where: $E_{\lambda ST}$ = the solar spectral irradiance inside the spacecraft (watts cm^{-2} sec^{-1} nm^{-1} x 10^{-7})

$E_{\lambda S}$ = solar spectral irradiance (watts cm^{-2} sec^{-1} nm^{-1} x 10^{-7})

T_{λ} = transmission of the optical transparency in decimal form

The results of these calculations for the APOLLO quartz window for the primate and human at each waveband from 210 nm to 320 nm are shown in Tables IV and V, column 4, $E_{\lambda T}$.

The moon spectral irradiance $E_{\lambda M}$ (Tables IV and V, column 5) was calculated by multiplying the solar spectral irradiance $E_{\lambda S}$ (column 2) by the reflectance of the moon's surface, r (assumed to be 3%):

$$E_{\lambda M} = E_{\lambda S} \cdot r$$

where: $E_{\lambda M}$ = moon spectral irradiance (watts cm^{-2} sec^{-1} nm^{-1} x 10^{-7})

$E_{\lambda S}$ = solar spectral irradiance on the moon's surface (watts cm^{-2} sec^{-1} nm^{-1} x 10^{-7})

r = reflectance factor of UV from moon's surface. Assumed to be .03.

The spectral irradiance of the moon inside the spacecraft was calculated as follows:

$$E_{\lambda MT} = E_{\lambda M} \cdot T_{\lambda}$$

$E_{\lambda MT}$ = moon irradiance inside the spacecraft

$E_{\lambda M}$ = moon spectral irradiance

T_{λ} = transmission of the intervening optical transparency in decimal form

These calculations are shown in Tables IV and V, column 6, for the APOLLO quartz spacecraft window.

The rate of irradiance inside the spacecraft for solar and moon irradiances for the quartz window at each waveband interval are shown in Tables IV and V, columns 9 (E_{SUV}) and 10 (E_{MUV}) respectively. Summing these columns and multiplying by the wavelength interval $\Delta\lambda$($\Delta\lambda$ = 10 nm) gives the total irradiance for the 210-320 nm spectrum within the spacecraft for each second, i.e., watts cm^{-2} sec^{-1} x 10^{-7}:

$$E_{SUV} = \sum_{320}^{210} E_{\lambda} T_{\lambda} W_{\lambda} \Delta\lambda$$

$$E_{MUV} = \sum_{320}^{210} E_{\lambda M} T_{\lambda} W_{\lambda} \Delta\lambda$$

where: E_{SUV} = solar radiant exposure (watts cm^{-2} sec^{-1} x 10^{-7})

E_{MUV} = moon radiant exposure (watts cm^{-2} sec^{-1} x 10^{-7})

$E_{\lambda S}$ = solar spectral irradiance (watts cm^{-2} sec^{-1} nm^{-1} x 10^{-7})

T_{λ} = transmission of spacecraft window in decimal form

W_{λ} = relative efficiency for photokeratitis at waveband λ

$\Delta\lambda$ = waveband interval of the spectrum ($\Delta\lambda$ = 10 nm)

All data necessary to calculate safe exposure time has been generated. The safe exposure time t is given by:

$$t = \frac{Q_{270}}{E_{SUV}} \text{ or } \frac{Q_{270}}{E_{MUV}}$$

where: t = safe exposure time in seconds

Q_{270} = radiant exposure threshold at 270 nm or 0.004 watts cm^{-2} for the primate or human

E_{SUV} = solar radiant exposure (watts cm^{-2} sec^{-1} x 10^{-7})

E_{MUV} = moon radiant exposure (watts cm^{-2} sec^{-1} x 10^{-7})

For the primate data given in Table IV, the safe exposure time from solar irradiance is as follows:

$$t_P = \frac{Q_{270}}{E_{SUV}} = \frac{.004 \text{ watts cm}^{-2}}{8214 \times 10^{-7} \text{ watts cm}^{-2} \text{ sec}^{-1}} = 4.9 \text{ sec}$$

For the human data given in Table V, the safe exposure time from solar irradiance is:

$$t_H = \frac{Q_{270}}{E_{SUV}} = \frac{.004 \text{ watts cm}^{-2}}{9964.9 \times 10^{-7} \text{ watts cm}^{-2} \text{ sec}^{-1}} = 4.01 \text{ sec}$$

This time means that with the quartz window directed toward the solar energy 4.01 seconds would be necessary before human photokeratitis symptoms would be observed after a latency period of 9 to 11 hours. Changing the angle of incidence of the solar irradiance on the quartz window would increase the safe exposure time t but data is not available for these calculations.

Safe exposure time from moon irradiance through the quartz window can be calculated as follows:

$$t_P = \frac{Q_{270}}{E_{MUV}} = \frac{0.004 \text{ watts cm}^{-2}}{251 \times 10^{-7} \text{ w cm}^{-2} \text{ sec}^{-1}} = 159.4 \text{ sec or } 2.7 \text{ min}$$

$$t_H = \frac{Q_{270}}{E_{MUV}} = \frac{0.004 \text{ watts cm}^{-2}}{309 \times 10^{-7} \text{ w cm}^{-2} \text{ sec}^{-1}} = 129.4 \text{ sec or } 2.2 \text{ min}$$

Lamplighter data given in Figure 17 indicates that the angle of incidence of the sun on the lunar surface has little effect on the reflectance of UV, i.e., the lunar surface acts as a Lambertian diffuser to ultraviolet. Thus, the lunar UV irradiance should be reasonably constant at modest angles of incidence on the spacecraft window.

It can be seen from these example calculations that under orbital conditions, with the spacecraft quartz window directed toward the sun,

additional protection would be needed if direct exposures to the cornea exceed about 5 seconds. The safe time from moon reflected UV would be extended to 2.7 minutes; however, combinations of moon and sun UV irradiance could reduce the 5 seconds value for sun exposure alone depending on the angle of incidence on the spacecraft window.

REFERENCES

1. Martin, E. K. The effects of ultraviolet rays upon the eye. Proc. Roy. Soc. (London), Series B, 85:319-323 (1912).
2. Duke-Elder, Sir W. S. Textbook of ophthalmology, Vol. 6. St. Louis, Mo.: C. V. Mosby Co., pp. 6443-6579, 1954.
3. Verhoeff, F. H., L. Bell, and C. B. Walker. The pathological effects of radiant energy on the eye. An experimental investigation with a systematic review on the literature. Proc. Amer. Acad. Arts and Sci. 51:630-811 (1916).
4. Buchanan, A. R., H. C. Heim, and D. W. Stilson. Biomedical effects of exposure to electromagnetic radiation. Part I. Ultraviolet. WADD Technical Report 60-376. Physics, Engineering, Chemistry Corporation, Boulder, Colorado, May 1960.
5. Bushke, W., J. S. Friedenwald, S. G. Moses. Effects of ultraviolet irradiation on corneal epithelium mitosis, nuclear fragmentation, post-traumatic cell movements, loss of tissue cohesion. J. Cell. Comp. Physiol. 26:147-164 (1945).
6. Cogan, D. G. and V. E. Kinsey. Action Spectrum of Keratitis Produced by Ultraviolet Radiation. Arch. Ophth. 35:670-677 (1946).
7. Kinsey, V. E. Spectral transmission of the eye to ultraviolet radiation. Arch. Ophthal. (Chicago) 39:508-513 (1948).
8. Bachem, A. Ophthalmic ultraviolet action spectra. Amer. J. Ophthal. 41:969-975 (1956).

9. Robinson, N. Solar radiation. New York, N. Y.: Elsevier Publishing Company, pp. 47-107, 1966.

10. Johnston, R. G., and R. P. Madden. On the use of thermopiles for absolute radiometry in the far ultraviolet. NBS Publication No. N66-33178, Washington, D. C., 1964.

11. Koller, L. R. Ultraviolet radiation, 2nd ed. New York, N. Y.: John Wiley and Sons, p. 298, 1965.

12. Watanabe, K. and C. Y. Inn. Intensity measurements in the vacuum ultraviolet. J.O.S.A. 43:32-35 (1953).

13. Pitts, Donald G. et al. The effects of ultraviolet radiation on the eye. SAM-TR-69-10, February 1969.

14. Pitts, Donald G., A comparative study of the effects of ultrabiolet radiation on the eye, SAM-TR-70-28, July 1970.

15. Brinkman, R. T., A. E. S. Green, and C. A. Barth. A digitalized solar ultraviolet spectrum. NASA Technical Report No. 32-951. Jet Propulsion Laboratory, Pasadena, California, August 1966,

16. Malitson, H. H., J. D. Purcell, R. Tousey, and C. E. Moore. The solar spectrum from 2635 to 2085 Å. Astrophysical J. 132:746-766 (1960).

17. Wilson, N., R. Tousey, J. D. Purcell, F. S. Johnson, and C. E. Moore. A revised analysis of the solar spectrum from 2990 to 2635 Å. Astrophysical J. 119:590-612 (1954).

18. Detwiler, C. R., D. L. Garret, J. D. Purcell, and R. Tousey. The intensity distribution in the UV solar spectrum. Ann. de Geophysique 17:263-272 (1961).

19. Johnson, F. S. Solar radiation. In Geotzel, C. G., J. B.

Rittenhouse, and J. B. Singletory (eds.). Space Material Handbook. Technical Documentary Report No. ML-TDR-64-40. Lockheed Missiles and Space Co., Sunnyvale, California, January 1965.

20. NASA Document 71.6158.1-009, page 8, 23 April 1971.

21. Lunar Bond Albedo Data in the Ultraviolet Region, from R. C. Stokes, Space Science Division, NASA, MSC.

TABLE I. Human Threshold Data for 9.9 nm Total Bandwidth

SUBJECT	E_e watts cm^{-2} sec^{-1} x 10^{-5}	T (sec)	Q watts cm^{-2} x 10^{-2}	CLASSIFICATION
		Waveband 220		
DWR	63.033	120	0.36	-
LBR	3.033	180	0.55	-
ACL	3.9	256	1.0	$+(Q_c)$
		Waveband 230		
ABR	24.9	32.0	0.8	-
JSR	24.9	40.0	1.0	-
RHL	28.4	45.5	1.3	$+(Q_c)$
		Waveband 240		
RMR	44.5	14.0	0.62	-
PCR	44.5	15.2	0.68	-
SQR	44.5	17.0	0.76	$+(Q_c)$
		Waveband 250		
PCL	65.7	12.2	0.8	$+(Q_c)$
APR	55.7	18.0	1.0	+
BBR	55.7	22.0	1.2	++
		Waveband 260		
ABR	111.3	4.9	0.55	-
RMR	111.3	5.8	0.65	-
DWR	111.3	6.7	0.75	$+(Q_c)$
		Waveband 270		
BAR	27.8	2.8	0.08	-
SR	28.9	4.4	0.13	-
APR	30.0	5.9	0.18	-
GSR	30.6	7.3	0.22	-
WBR	30.0	9.9	0.30	$\pm$
SQL	50.0	7.0	0.35	$\pm$
BWV	111.3	3.6	0.40	$\pm(Q_c)$

TABLE I (Continued)

SUBJECT	E_e watts cm^{-2} sec^{-1} x 10^{-5}	T (sec)	Q watts cm^{-2} x 10^{-2}	CLASSIFICATION
		Waveband 280		
GCL	122.0	3.8	0.46	-
GP	69.3	7.5	0.52	$\pm$
BBL	169.0	3.5	0.59	$\pm(Q_c)$
DML	413.0	2.3	0.95	$\pm\pm$
		Waveband 290		
GCR	94.6	4.8	0.46	-
DWL	94.6	5.8	0.55	-
APL	80.7	7.8	0.63	$\pm$
SQL	77.9	8.3	0.65	$\pm$
RCR	105.7	6.6	0.70	$\pm(Q_c)$
		Waveband 300		
JBR	77.9	5.6	0.44	-
FGL	77.9	7.0	0.55	-
SRR	89.0	7.4	0.66	-
BVL	105.7	6.6	0.70	$+(Q_c)$
		Waveband 310		
PAL	94.6	8.5	0.80	-
RML	94.6	10.0	0.95	-
RHR	125.2	9.5	1.2	-
BCL	155.8	9.0	1.4	$+(Q_c)$

TABLE II. Criteria and Subject's Responses for Different Wavebands. Threshold was taken as five positive responses for the different criteria. Scatter measurements were not made in early experiments.

SUBJECTS	CRITERIA							
	EPITHELIAL DEBRIS	EPITHELIAL HAZE	GRANULES	PHOTOPHOBIA	VISUAL ACUITY	SYMPTOMS	SCATTER	CLASSIFI-CATION
				Waveband 220				
DWR	+	−	−	−	±	±	+	−
LBR	+	−	−	−	−	−	+	−
ACL	‡	‡	+	±	+	+	‡	++
				Waveband 230				
ABR	+	−	−	−	−	−	±	−
JSR	+	−	±	−	−	−	±	−
RHL	+	+	±	±	+	+	+	+
				Waveband 240				
RMR	+	±	−	−	−	−	+	−
PCR	+	±	−	−	−	−	+	−
SQR	+	+	+	−	+	+	+	+
				Waveband 250				
PCL	+	+	‡	±	+	+	+	+
APR	+	+	‡	±	−	+	+	++
BBR	‡	+	+	+	‡	‡	+	+++
				Waveband 260				
ABR	+	±	−	−	−	−	+	−
RR	+	±	±	−	−	−	+	−
DR	+	+	±	±	+	+	+	+
				Waveband 270				
AR	±	−	−	−	−	−		−
SR	±	−	−	−	−	−		−
APR	±	±	−	−	±	−		−
GSR	+	±	±	−	−	±		−
WBR	+	+	±	−	±	−	+	±

TABLE II (Continued)

SUBJECTS	CRITERIA							
	EPITHELIAL DEBRIS	EPITHELIAL HAZE	GRANULES	PHOTOPHOBIA	VISUAL ACUITY	SYMPTOMS	SCATTER	CLASSIFI-CATION
				Waveband 270				
SL	+	+	+	−	−	−	+	+
BVR	+	+	+	−	+	−	+	+
				Waveband 280				
GCL	−	−	−	−	−	−		−
GPL	+	+	+	+	+	+	+	+
BBL	+	+	+	+	+	+		+
DML	+	+	+	+	+	+		+
				Waveband 290				
GCR	+	−	−	−	−	−	−	−
DWL	+	+	+	−	+	−	+	−
APL	+	+	+	+	+	+	+	+
SQL	+	+	−	−	−	+	+	+
RCR	+	+	+	+	−	+	+	+
				Waveband 300				
JBR	+	−	−	−	−	−	+	−
FGL	+	+	−	−	+	+	+	−
SRR	+	+	+	−	−	−	+	−
BVL	+	+	+	−	+	−	+	+
				Waveband 310				
PAL	+	+	−	−	−	−	+	−
RML	+	+	−	−	−	−	+	−
RHR	+	+	+	−	−	+	+	−
BCL	+	+	+	+	+	+	+	+

TABLE III. Summary of Photokeratitis Thresholds for Rabbits, Primates and Humans

Waveband in nm	Rabbit			Primate			Human		
	Radiant Exposure Threshold		Relative Efficiency	Radiant Exposure Threshold		Relative Efficiency	Radiant Exposure Threshold		Relative Efficiency
	ergs cm^{-2} x 10^{6}	watts cm^{-2} x 10^{-2}		ergs cm^{-2} x 10^{6}	watts cm^{-2} x 10^{-2}		ergs cm^{-2} x 10^{6}	watts cm^{-2} x 10^{-2}	
205-215	7.00	70.	0.007	3.27	32.7	0.012	----	----	----
215-225	0.46	4.6	0.11	0.21	2.1	0.19	0.1	1.0	0.40
225-235	0.30	3.0	0.17	0.22	2.2	0.18	0.13	1.3	0.31
235-245	0.33	3.3	0.15	0.12	1.2	0.33	0.07	0.76	0.53
245-255	0.41	4.1	0.12	0.20	2.0	0.20	0.08	0.80	0.50
255-265	0.18	1.8	0.28	0.11	1.1	0.36	0.75	0.75	0.53
265-275	0.05	0.5	1.00	0.04	0.4	1.00	0.04	0.40	1.00
275-285	0.11	1.1	0.45	0.06	0.6	0.67	0.059	0.59	0.68
285-295	0.12	1.2	0.42	0.07	0.7	0.57	0.07	0.70	0.57
295-305	0.22	2.2	0.23	0.11	1.1	0.36	0.17	0.70	0.57
305-315	0.47	4.7	0.11	0.20	2.0	0.20	0.14	1.40	0.29
315-325	6.00	60.	0.008	3.5	35.0	0.011	----	----	----
325-335	50.0	500.	----	----	----	----	----	----	----
345-355	50.0	500.	----	----	----	----	----	----	----

TABLE IV. Calculation of Safe Exposure Duration for UV Using Primate Data

WAVELENGTH nm	SOLAR SPECTRAL IRRADIANCE ($E_{\lambda S}$) watts $cm^{-2}sec^{-1}nm^{-1}$ x 10^{-7}	TRANSMISSION APOLLO WINDOW T_λ (in decimal)	SOLAR IRRADIANCE INSIDE SPACECRAFT $E_{\lambda ST}$ ($E_{\lambda S} \cdot T_\lambda$) watts $cm^{-2}sec^{-1}nm^{-1}$ x 10^{-7}	MOON SPECTRAL IRRADIANCE ($E_{\lambda M}$) watts $cm^{-2}sec^{-1}nm^{-1}$ x 10^{-7}	MOON IRRADIANCE INSIDE SPACECRAFT $E_{\lambda MT} = E_{\lambda M} \cdot T_\lambda$	PRIMATE RADIANT THRESHOLD EXPOSURE Q_{CP} watts cm^{-2}	PRIMATE RELATIVE EFFICIENCY $W_{\lambda P} = \frac{Q_{270}}{Q_{CP(\lambda)}}$	E_{SUV} ($E_{\lambda S} W_\lambda T_\lambda$) watts $cm^{-2}sec^{-1}nm^{-1}$ x 10^{-7}	E_{MUV} ($E_{\lambda M} W_\lambda T_\lambda$) watts $cm^{-2}sec^{-1}nm^{-1}$ x 10^{-7}
210	30.3	.36	10.9	0.9	.32	.327	.012	0.131	.004
220	43.5	.44	19.1	1.3	.57	.021	.19	4.0	.11
230	59.2	.52	30.8	2.0	1.0	.022	.18	5.5	.18
240	59.4	.54	32.1	2.0	1.1	.012	0.33	10.6	.36
250	67.7	.63	42.7	2.0	1.3	.020	0.20	8.5	.26
260	132.2	.70	92.5	5.0	3.5	.011	0.36	33.3	1.26
270	256.2	.70	179.3	8.0	5.6	.004	1.00	179.3	5.6
280	210.4	.70	147.3	6.3	4.4	.006	0.67	98.7	2.95
290	538.3	.70	376.8	16.0	11.2	.007	0.57	214.8	6.38
300	610.0	.70	427.0	18.0	12.6	.011	0.36	153.7	4.54
310	760.0	.70	532.0	23.0	16.1	.020	0.20	106.4	3.22
320	850.0	.70	595.0	26.0	18.2	.35	0.011	6.5	.20

$\sum_{320}^{210} E_{SUV} \cdot \Delta\lambda = 8.214 \times 10^{-7}$ watts $cm^{-2}sec^{-1}$; $\sum_{320}^{210} E_{MUV} \cdot \Delta\lambda = 251 \times 10^{-7}$ watts $cm^{-2}sec^{-1}$

TABLE V. Calculation of Safe Exposure Duration for UV Using Human Data

WAVELENGTH nm	SOLAR SPECTRAL IRRADIANCE ($E_{\lambda S}$) watts $cm^{-2}sec^{-1}nm^{-1}$ x 10^{-7}	TRANSMISSION APOLLO WINDOW T_λ (in decimal)	SOLAR IRRADIANCE INSIDE SPACECRAFT $E_{\lambda ST}$ ($E_{\lambda S} \cdot T_\lambda$) watts $cm^{-2}sec^{-1}nm^{-1}$ x 10^{-7}	MOON SPECTRAL IRRADIANCE ($E_{\lambda M}$) watts $cm^{-2}sec^{-1}nm^{-1}$ x 10^{-7}	MOON IRRADIANCE INSIDE SPACECRAFT $E_{\lambda MT} = E_{\lambda M} \cdot T_\lambda$	PRIMATE RADIANT THRESHOLD EXPOSURE Q_{CH} watts cm^{-2}	PRIMATE RELATIVE EFFICIENCY $W_{\lambda H} = \frac{Q_{270}}{Q_{CH(\lambda)}}$	E_{SUV} ($E_{\lambda S} W_\lambda T_\lambda$) watts $cm^{-2}sec^{-1}nm^{-1}$ x 10^{-7}	M_{SUV} ($E_{\lambda M} W_\lambda T_\lambda$) watts $cm^{-2}sec^{-1}nm^{-1}$ x 10^{-7}
210	30.3	.36	10.9	0.9	.32	----	----	------	----
220	43.5	.44	19.1	1.3	.57	.010	0.40	7.64	.23
230	59.2	.52	30.8	2.0	1.0	.013	0.31	9.55	.31
240	59.4	.54	32.1	2.0	1.1	.008	0.53	17.01	.58
250	67.7	.63	42.7	2.0	1.3	.008	0.50	21.35	.65
260	132.2	.70	92.5	5.0	3.5	.008	0.53	49.03	1.86
270	256.2	.70	179.3	8.0	5.6	.004	1.00	179.30	5.60
280	210.4	.70	147.3	6.3	4.4	.006	0.68	100.16	2.99
290	538.3	.70	376.8	16.0	11.2	.007	0.57	214.78	6.83
300	610.0	.70	427.0	18.0	12.6	.007	0.57	243.39	7.18
310	760.0	.70	532.0	23.0	16.1	.014	0.29	154.28	4.67
320	850.0	.70	595.0	26.0	18.2	----	----	------	----

$\sum_{310}^{220} E_{SUV} \cdot \Delta\lambda = 9964.9 \times 10^{-7}$ watts $cm^{-2}sec^{-1}$; $\sum_{310}^{220} M_{SUV} \cdot \Delta\lambda = 309 \times 10^{-7}$ watts $cm^{-2}sec^{-1}$

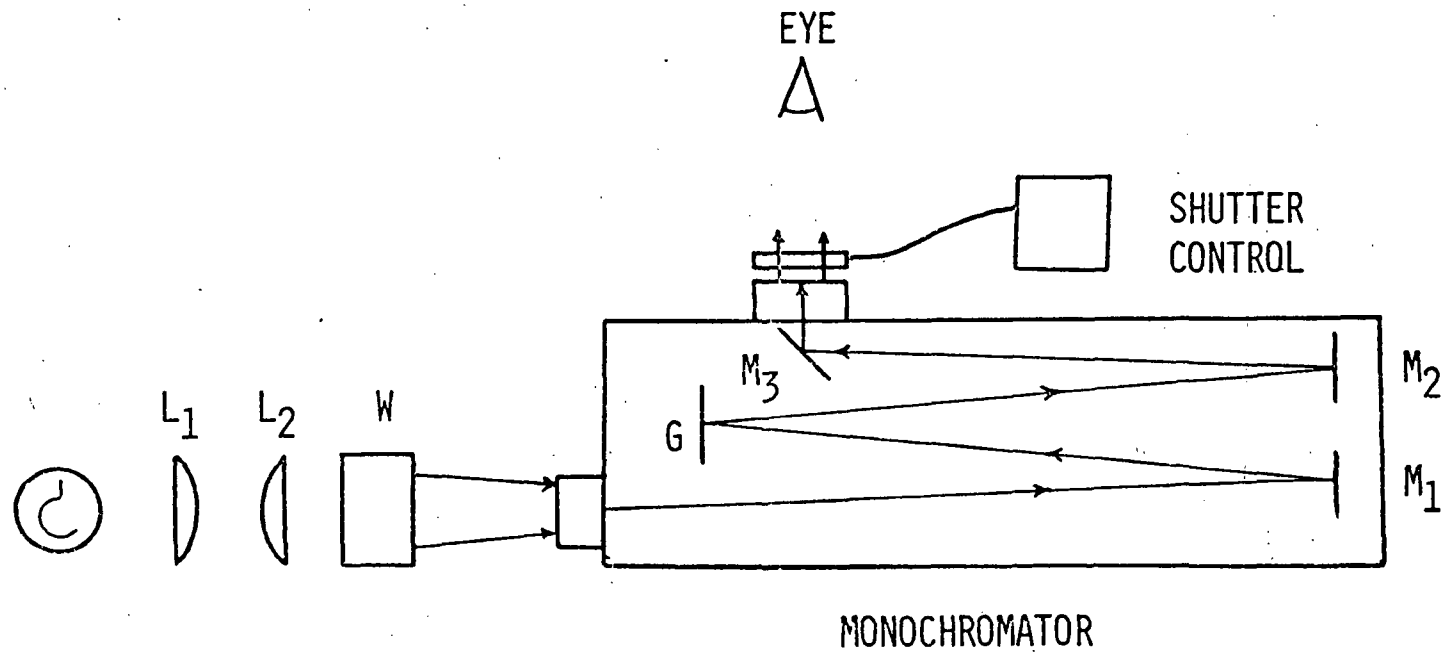

FIGURE 1. SCHEMATIC OF UV SOURCE AND EXPOSURE APPARATUS

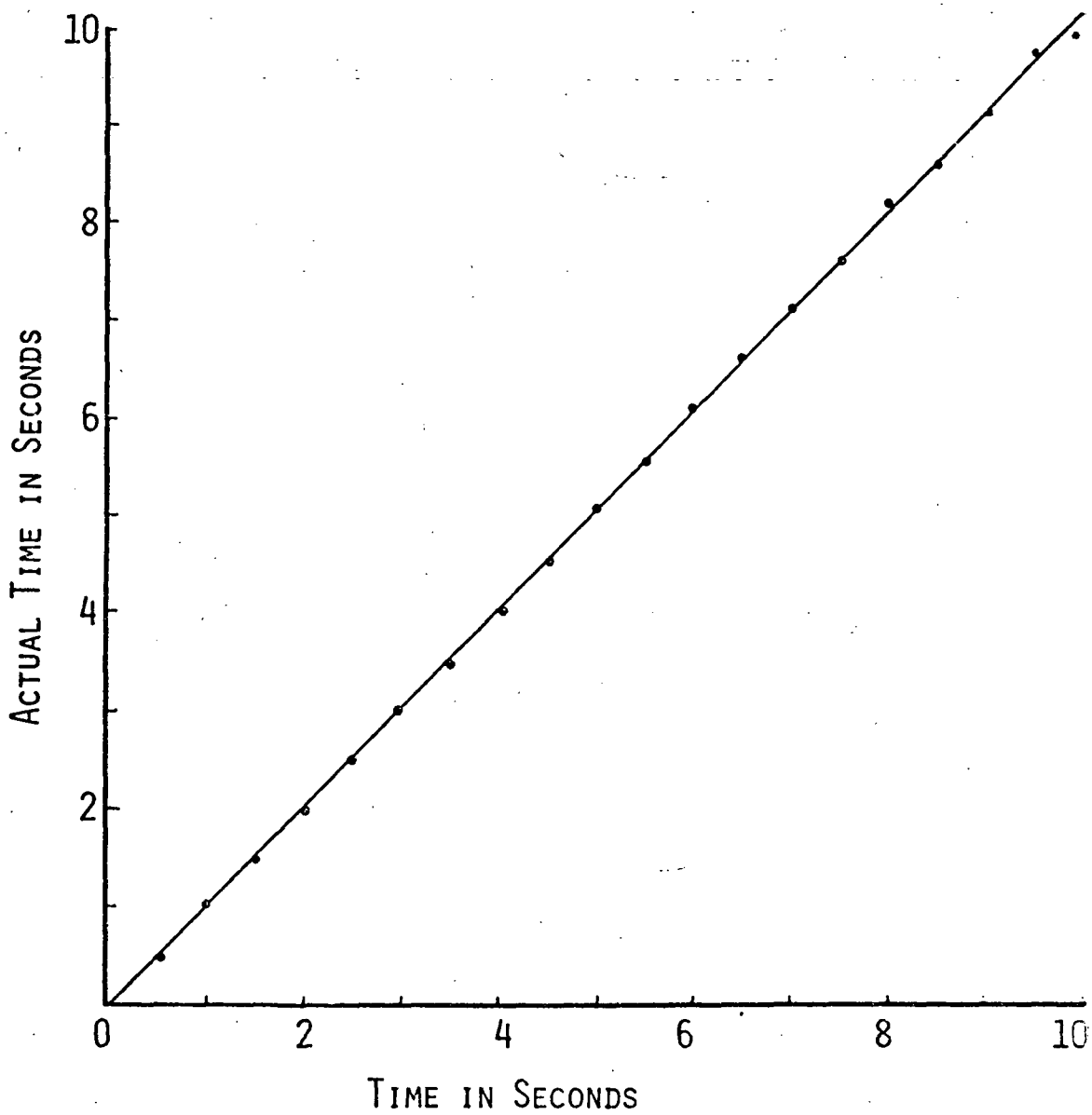

FIGURE 2. CALIBRATION CURVE OF THE ELECTRONIC SHUTTER. THE ORDINATE GIVES THE TIME READ FROM THE OSCILLOSCOPE PHOTOGRAPH AND THE ABSCISSA THE SHUTTER TIME.

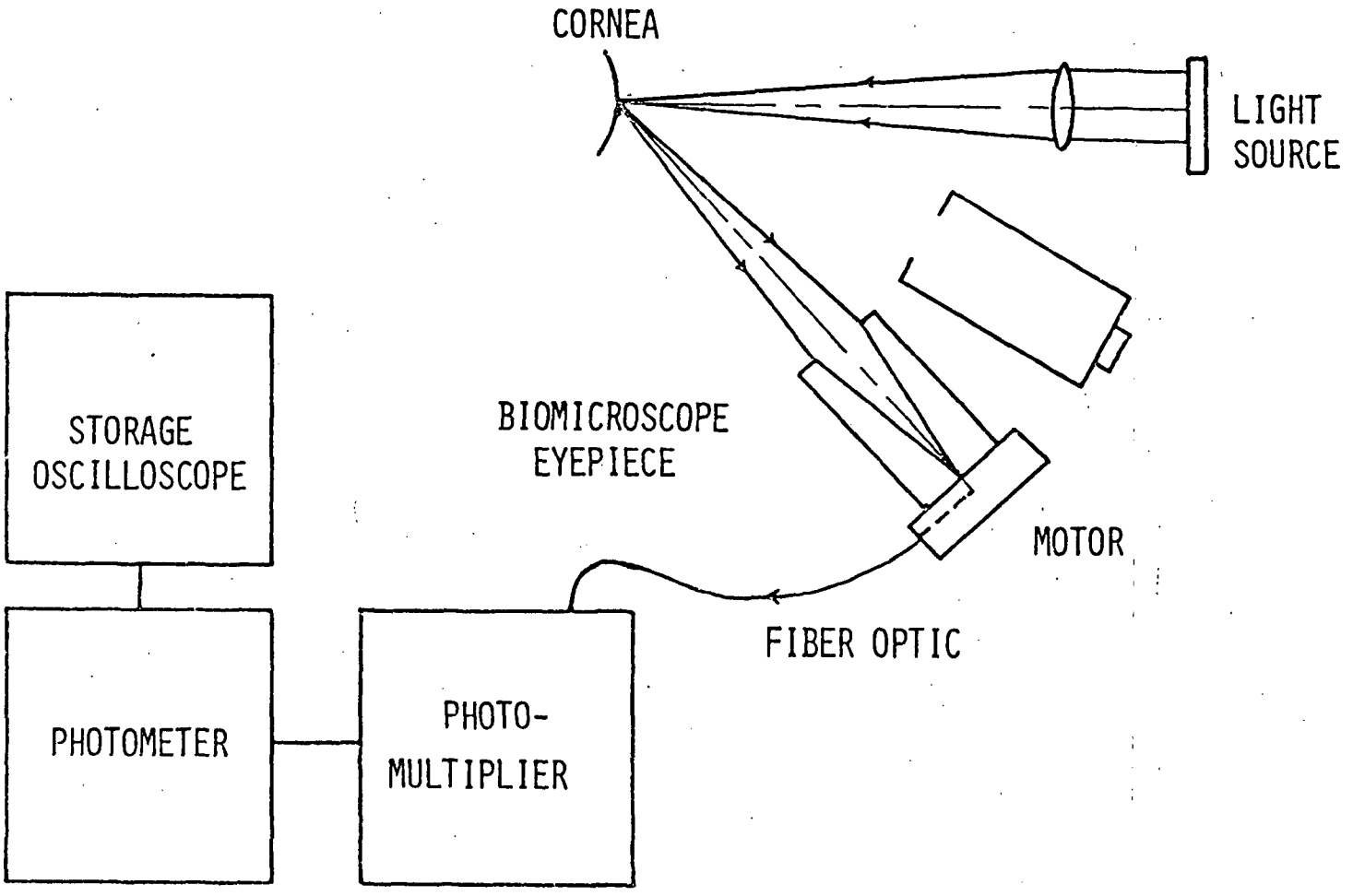

FIGURE 3. SCHEMATIC OF CORNEAL LIGHT SCATTER MEASUREMENT APPARATUS

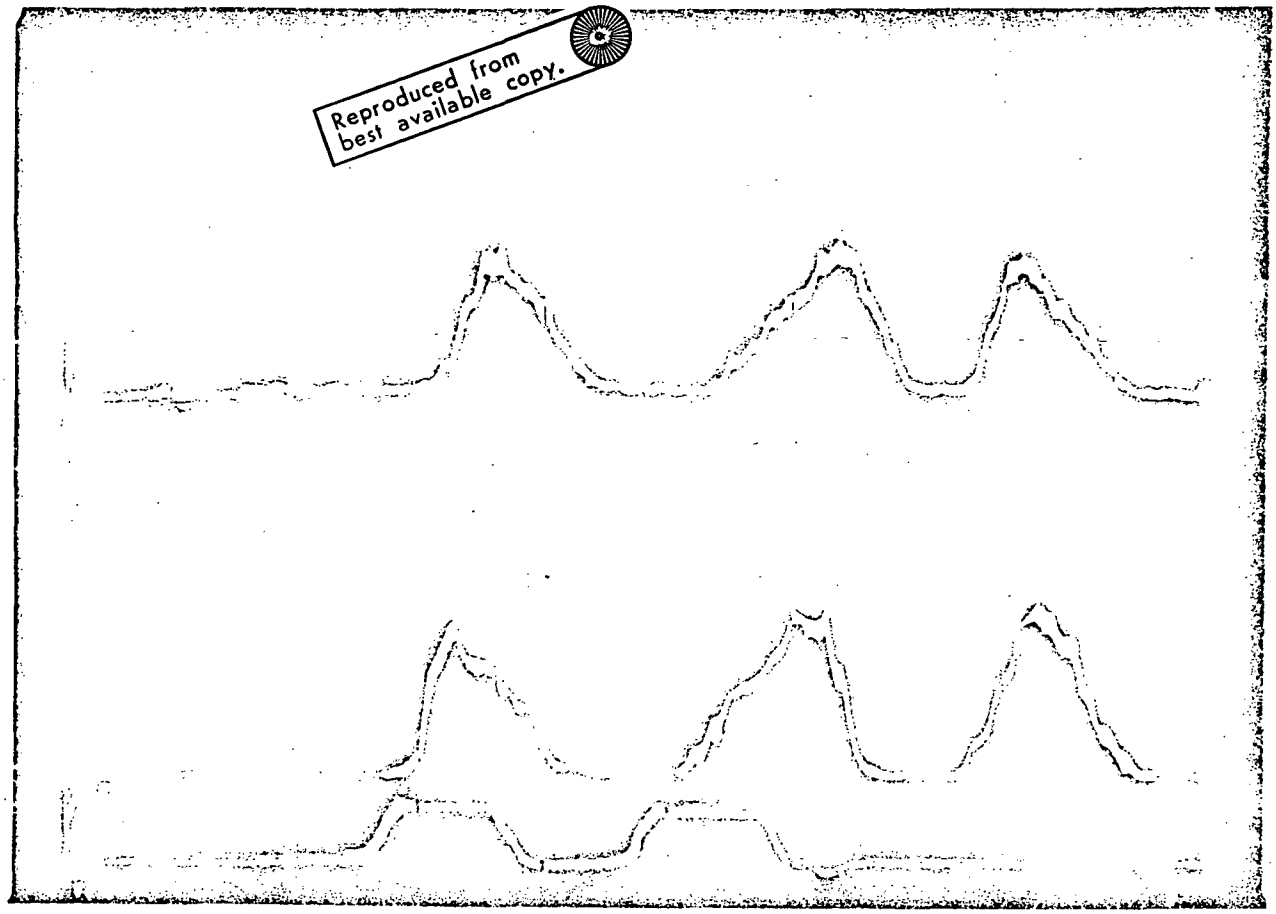

FIGURE 4. CORNEAL LIGHT SCATTER TRACES FROM THE HUMAN EYE. THE LOWER TRACE IDENTIFIED THE SUBJECT. THE MIDDLE AND UPPER TRACES REPRESENT CORNEAL LIGHT SCATTER MEASUREMENTS. SCATTER WAS MEASURED FROM EPITHELIUM TO ENDOTHELIUM THEN REVERSED. THE FIRST MEASUREMENT OF THE MIDDLE TRACE REPRESENTS THE IDEAL CURVE. SMALL WIGGLES IN EACH TRACE ARE CAUSED BY EYE MOVEMENTS. THE AMPLITUDE OF EACH SCATTER CURVE WAS DETERMINED AND A PERCENT SCATTER CHANGE FROM PRE-EXPOSURE BASELINE DATA WAS CALCULATED FOR PLOTTING.

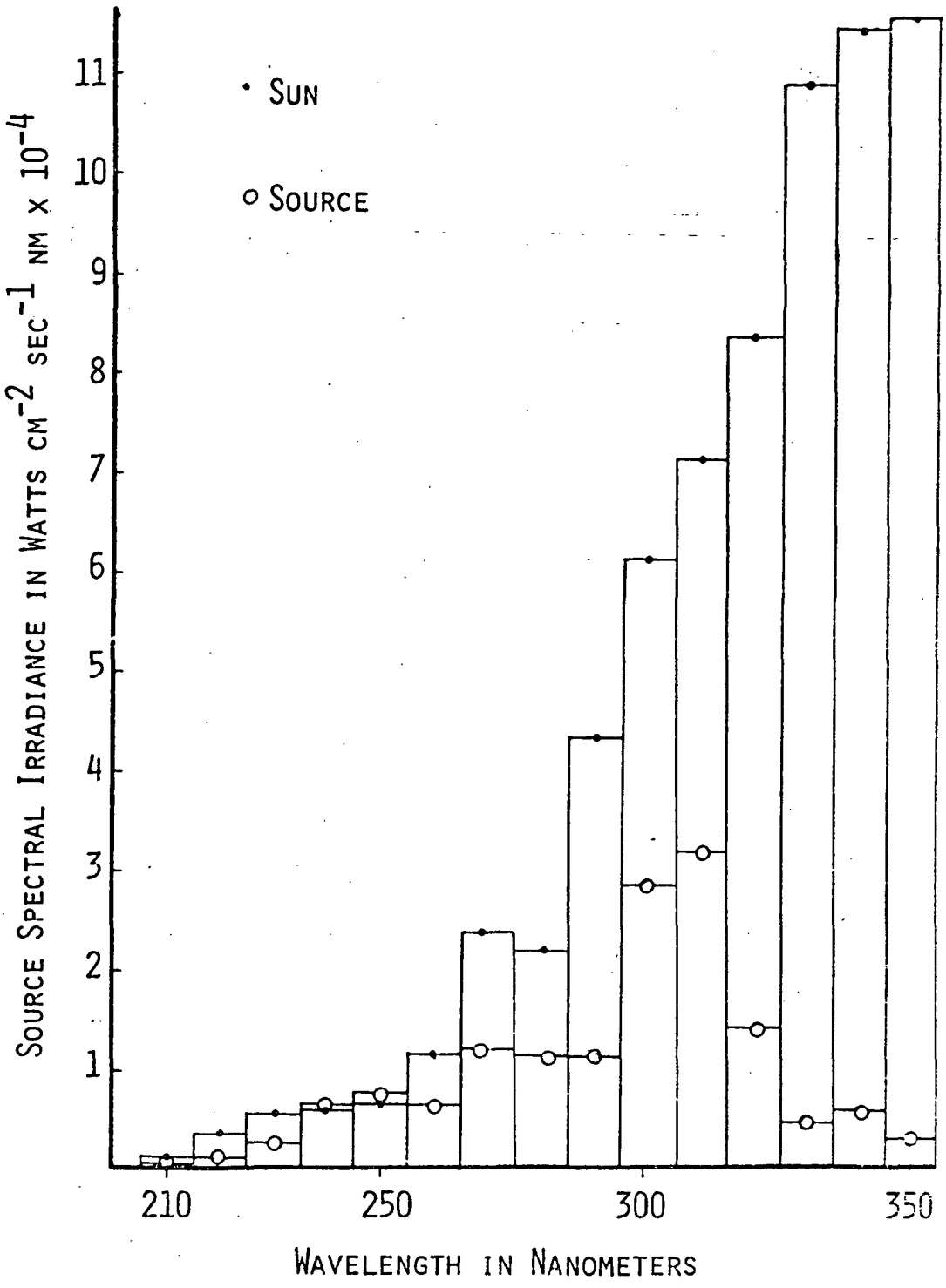

FIGURE 5. Comparison of Solar and Source Ultraviolet Irradiance.

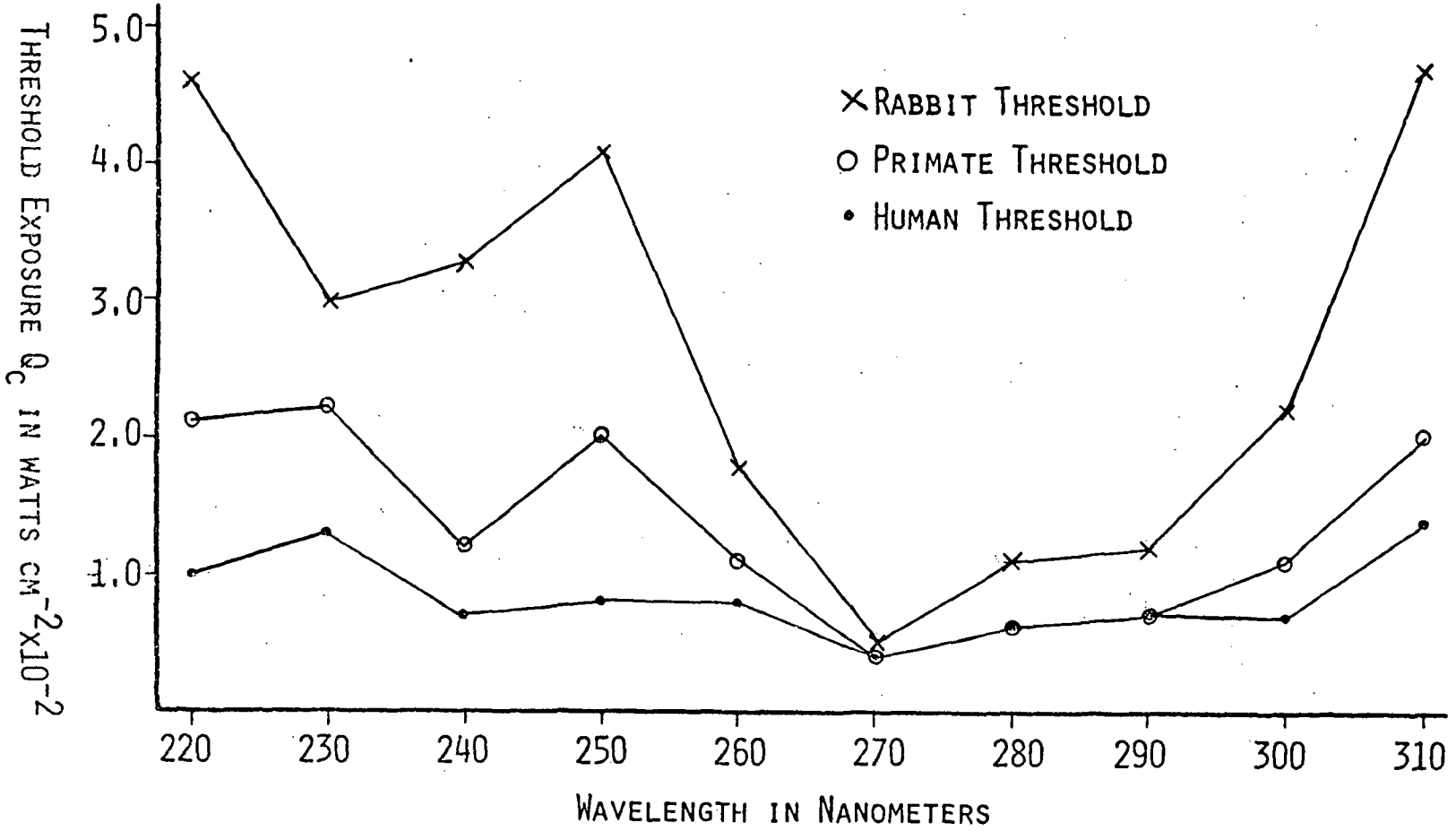

FIGURE 6. COMPARISON OF THE ULTRAVIOLET ACTION SPECTRUM FOR THE RABBIT, PRIMATE AND HUMAN

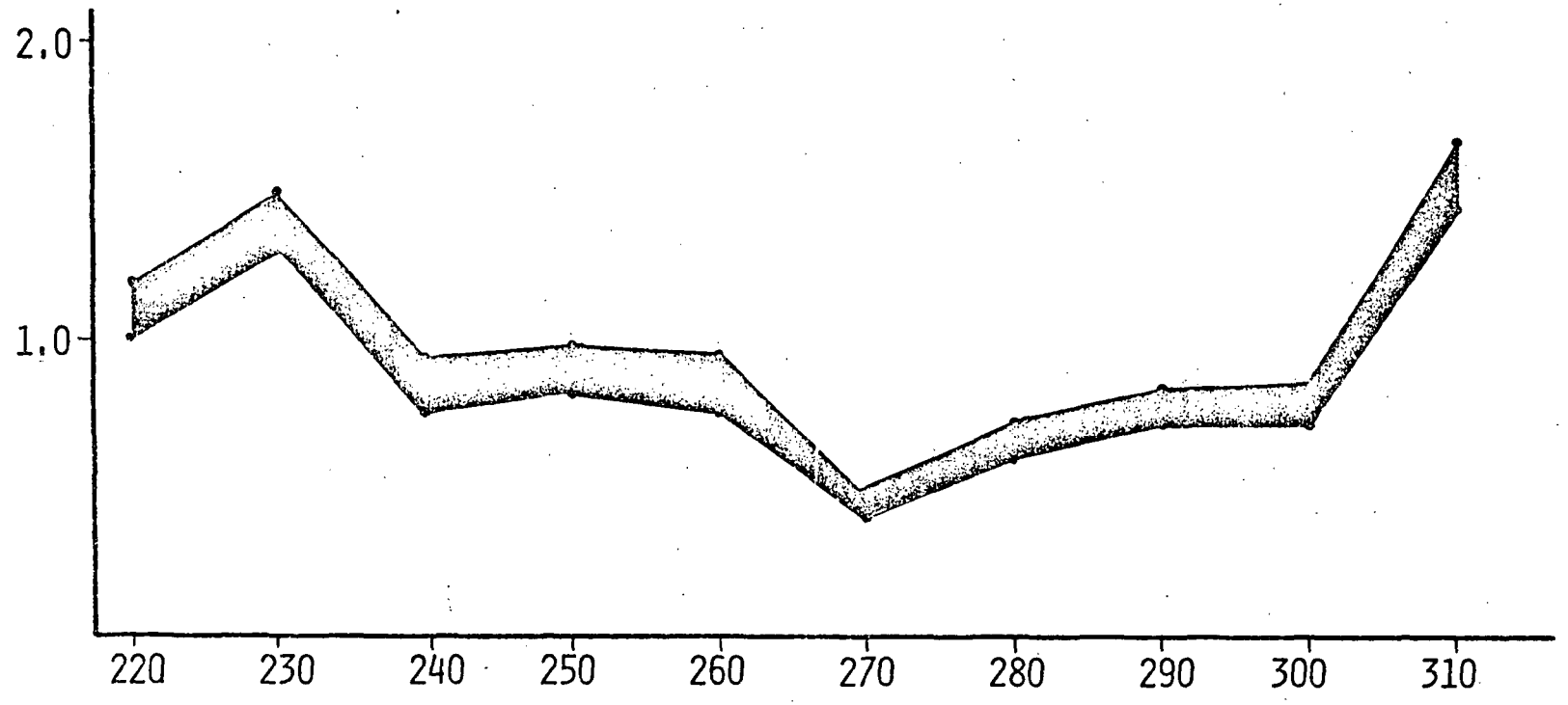

FIGURE 7. HUMAN ULTRAVIOLET EXPOSURE LIMITS. THE LOWER CURVE PRESENTS THE THRESHOLD RADIANT EXPOSURE FOR THE HUMAN. THE UPPER CURVE IS 20% ABOVE THRESHOLD AND INDICATES THE LEVEL OF ULTRAVIOLET REQUIRED FOR DISCOMFORT AND INCAPACITATION.

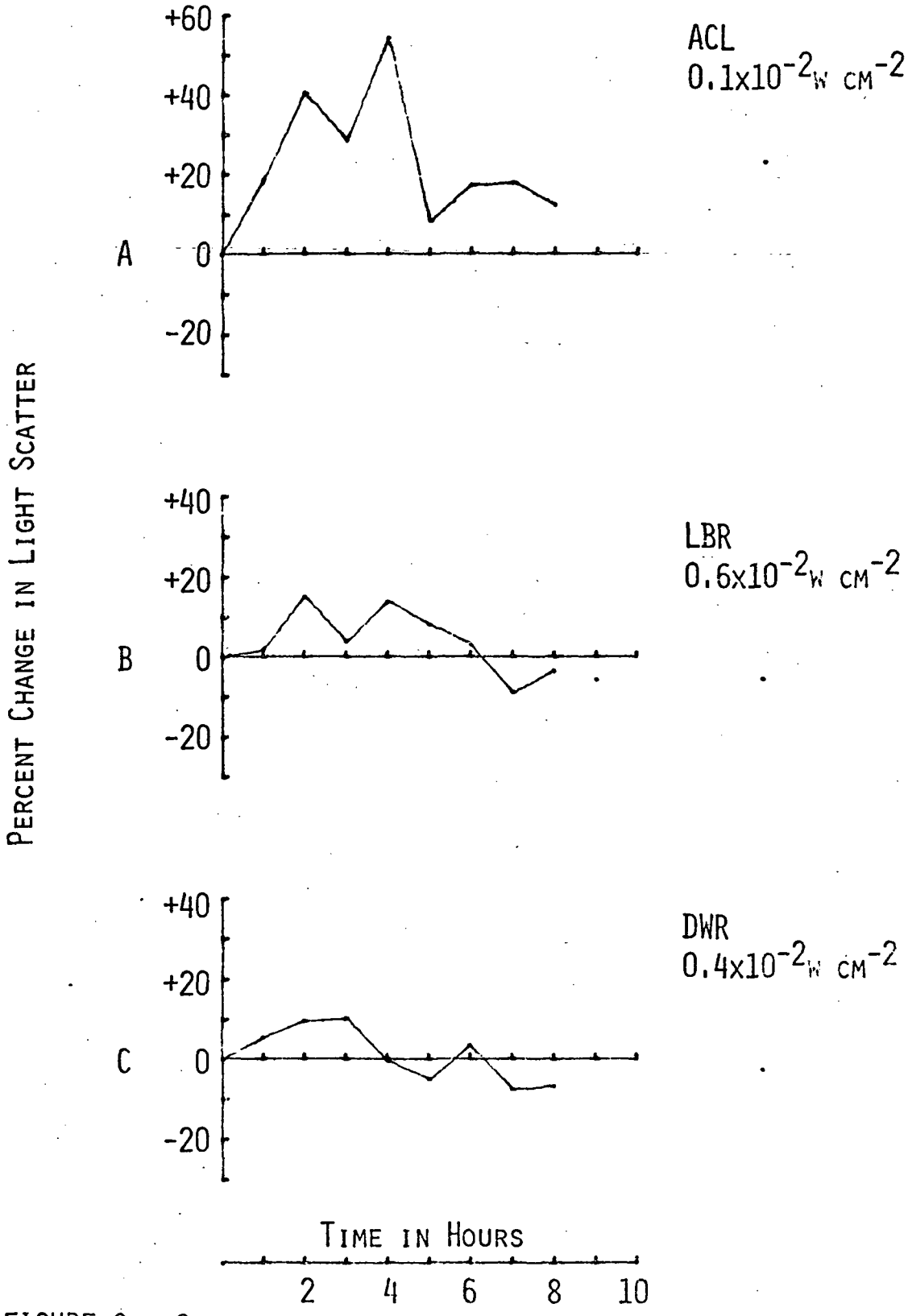

FIGURE 8. CORNEAL LIGHT SCATTER MEASUREMENTS FOR WAVEBAND 220 NM. SUBJECT CODE AND RADIANT EXPOSURE ARE INDICATED BY EACH GRAPH. THE SINGLE POINT TO THE RIGHT OF THE GRAPH INDICATES THE PERCENT CHANGE IN SCATTER 24 HOURS POST EXPOSURE

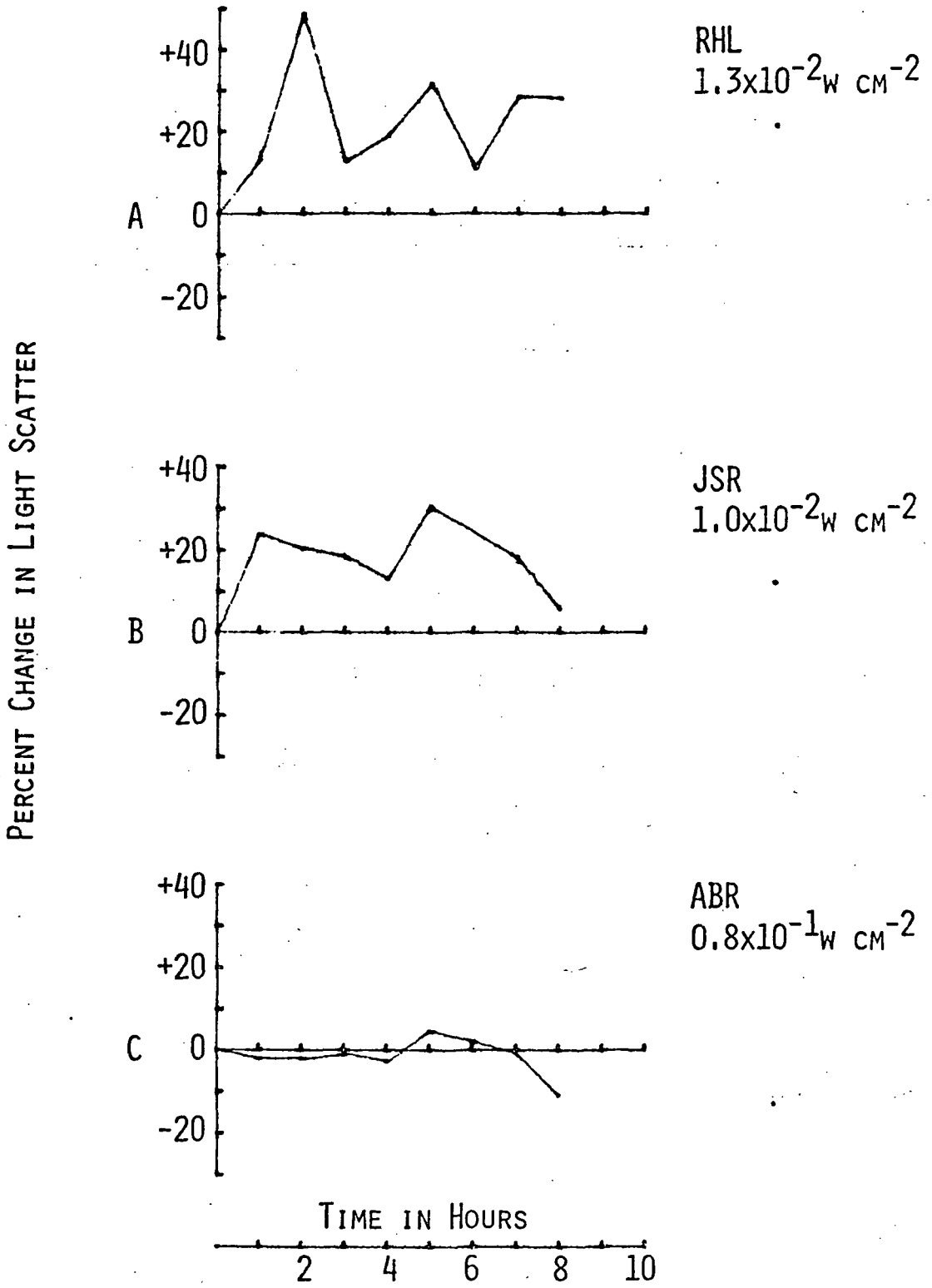

FIGURE 9. CORNEAL LIGHT SCATTER MEASUREMENTS FOR WAVEBAND 230 NM. SUBJECT CODE AND RADIANT EXPOSURE ARE INDICATED BY EACH GRAPH. THE SINGLE POINT TO THE RIGHT OF THE GRAPH INDICATES THE PERCENT CHANGE IN SCATTER 24 HOURS POST EXPOSURE.

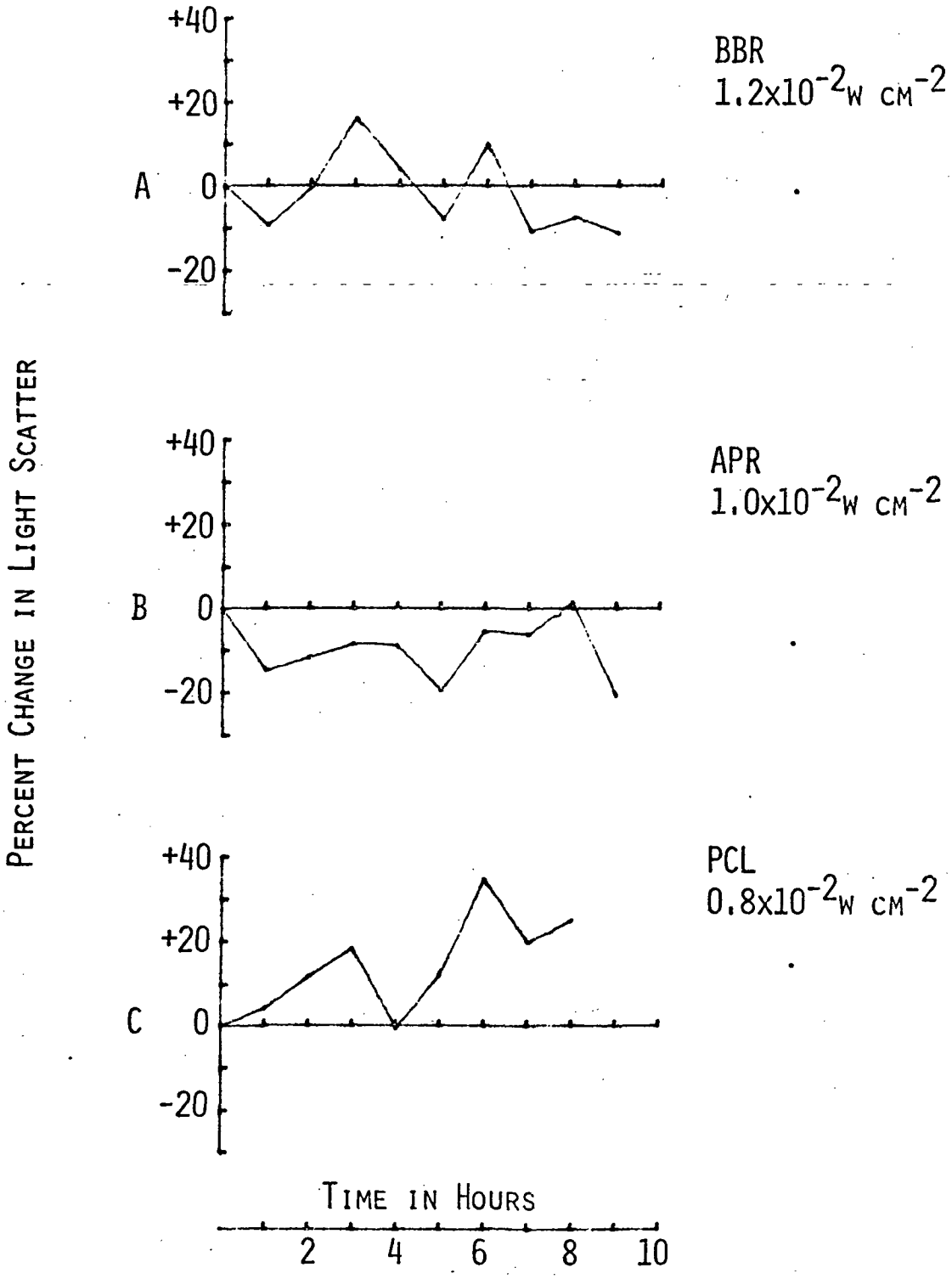

FIGURE 10. CORNEAL LIGHT SCATTER MEASUREMENTS FOR WAVEBAND 250 NM. SUBJECT CODE AND RADIANT EXPOSURE ARE INDICATED BY EACH GRAPH. THE SINGLE POINT TO THE RIGHT OF THE GRAPH INDICATES THE PERCENT CHANGE IN SCATTER 24 HOURS POST EXPOSURE.

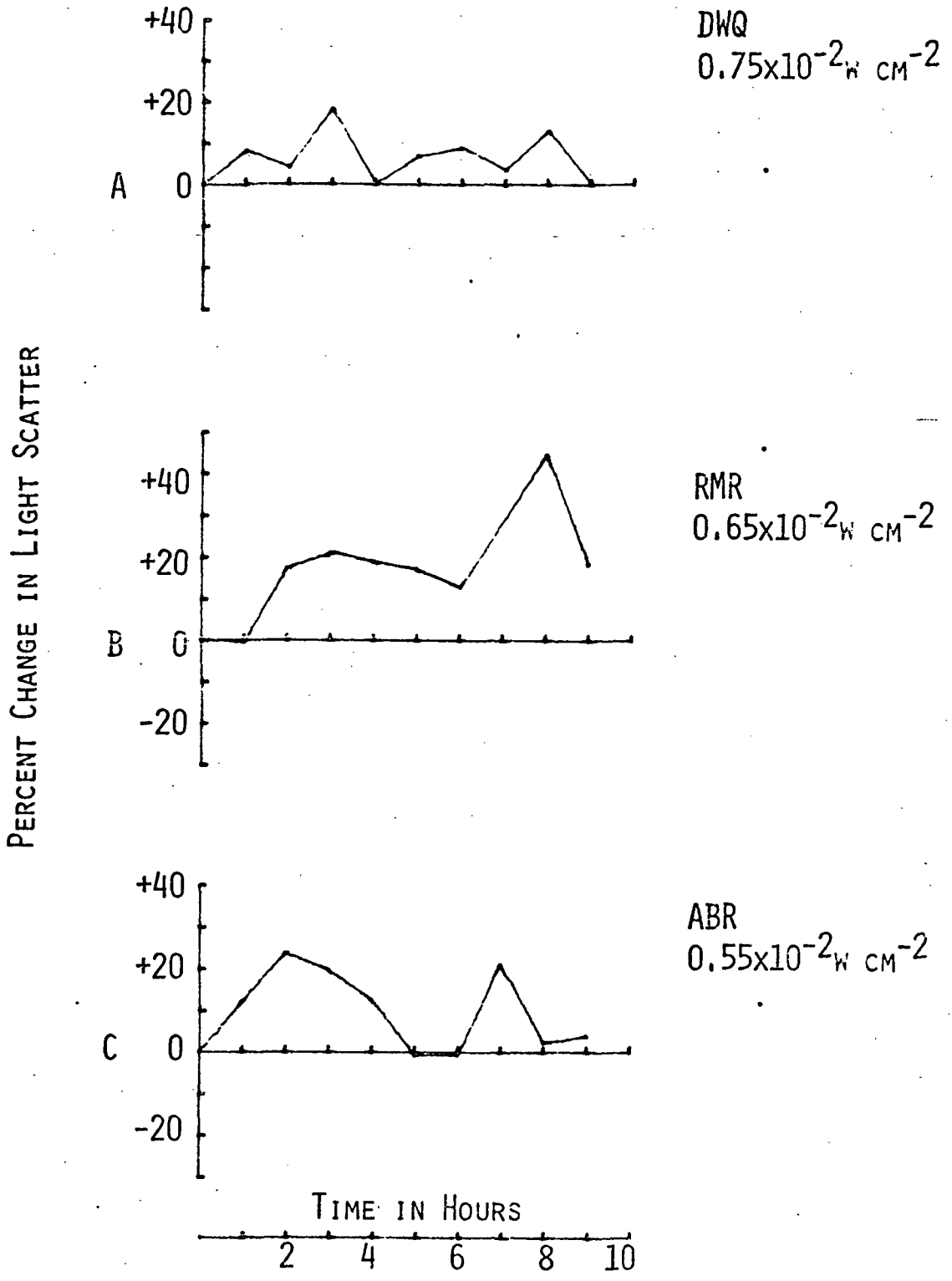

FIGURE 11. CORNEAL LIGHT SCATTER MEASUREMENTS FOR WAVEBAND 260 NM. SUBJECT CODE AND RADIANT EXPOSURE ARE INDICATED BY EACH GRAPH. THE SINGLE POINT TO THE RIGHT OF THE GRAPH INDICATES THE PERCENT CHANGE IN SCATTER 24 HOURS POST EXPOSURE.

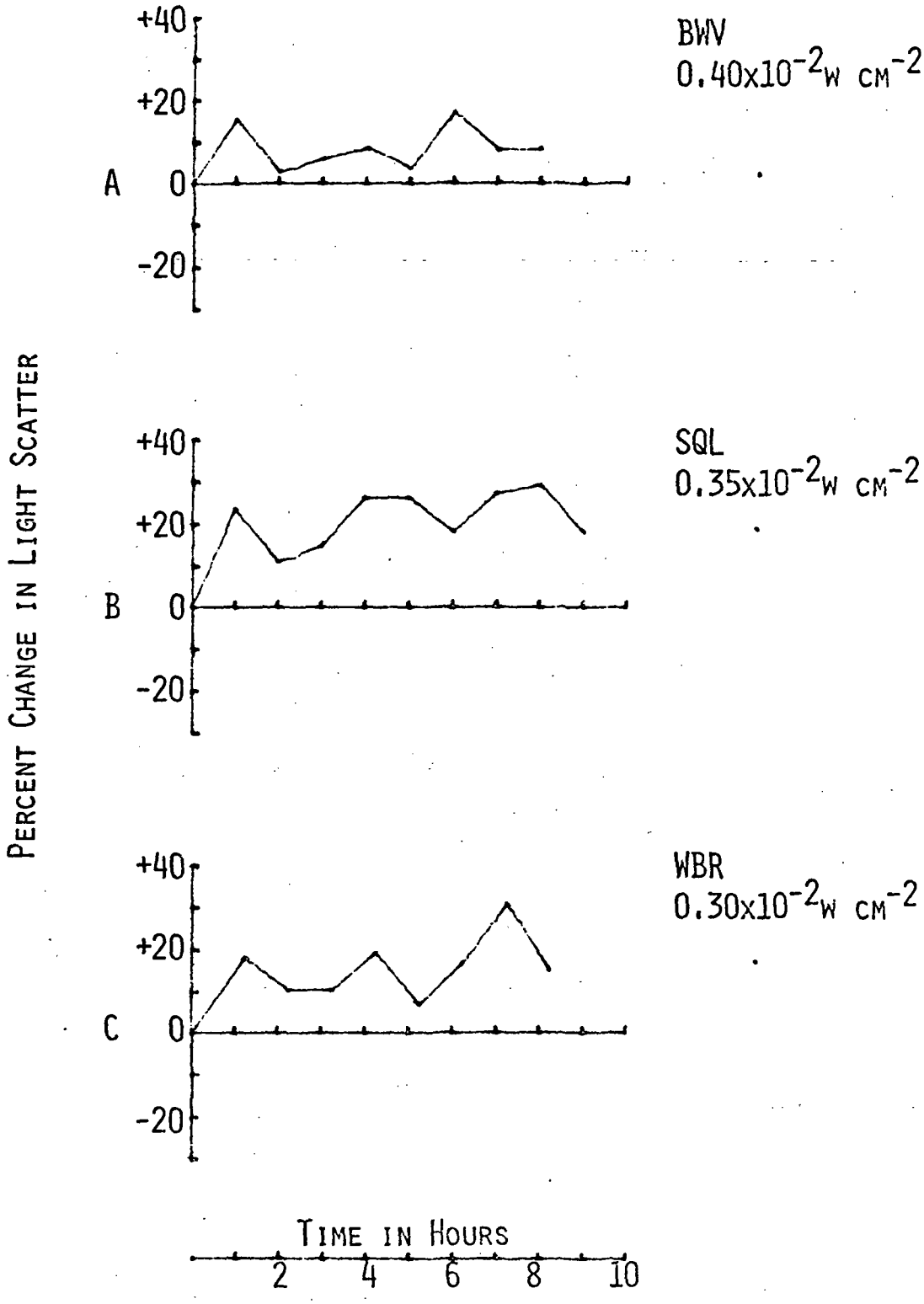

FIGURE 12. CORNEAL LIGHT SCATTER MEASUREMENTS FOR WAVEBAND 270 NM. SUBJECT CODE AND RADIANT EXPOSURE ARE INDICATED BY EACH GRAPH. THE SINGLE POINT TO THE RIGHT OF THE GRAPH INDICATES THE PERCENT CHANGE IN SCATTER 24 HOURS POST EXPOSURE.

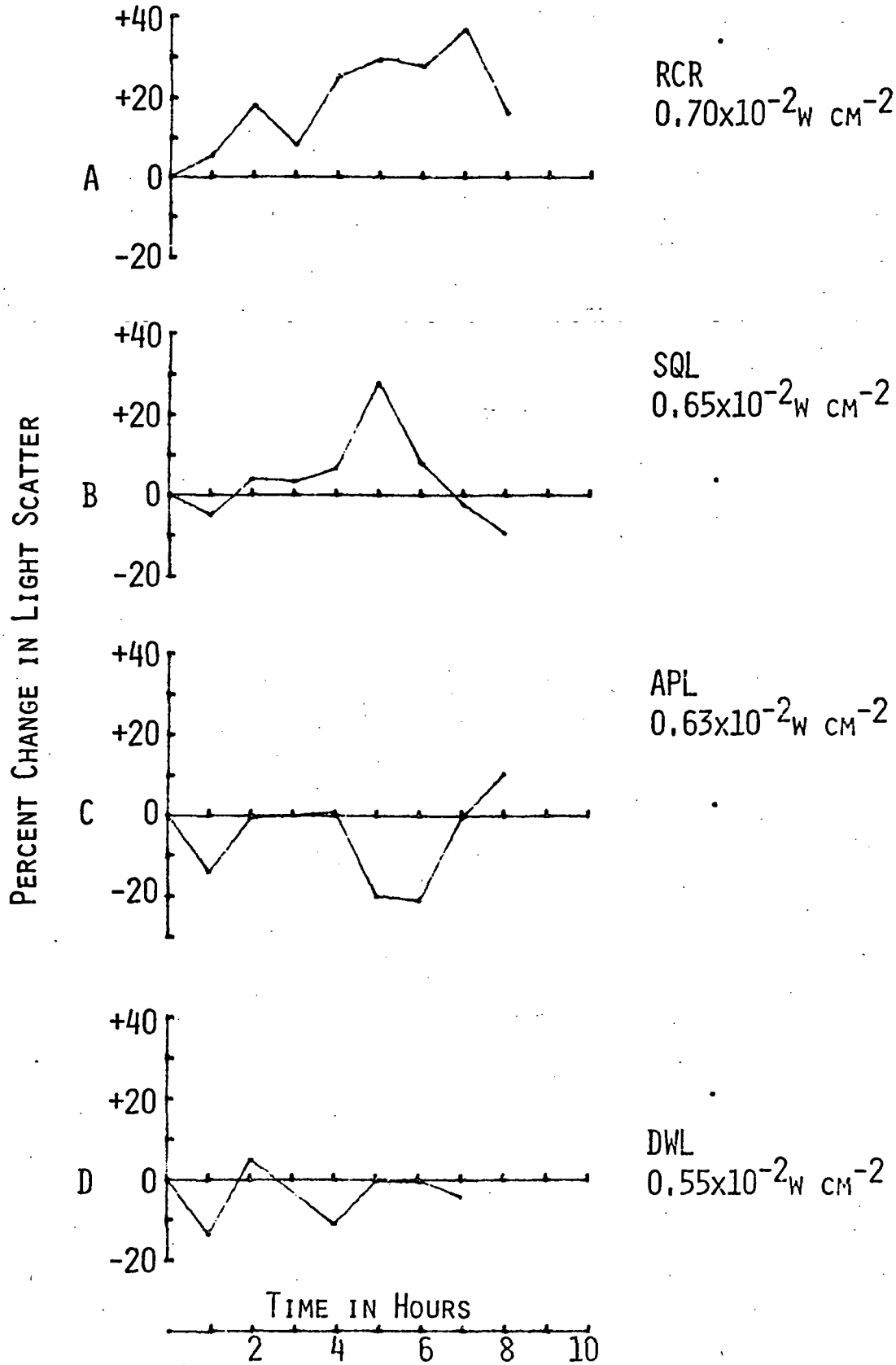

FIGURE 13. CORNEAL LIGHT SCATTER MEASUREMENTS FOR WAVEBAND 290 NM. SUBJECT CODE AND RADIANT EXPOSURE ARE INDICATED BY EACH GRAPH. THE SINGLE POINT TO THE RIGHT OF THE GRAPH INDICATES THE PERCENT CHANGE IN SCATTER 24 HOURS POST EXPOSURE.

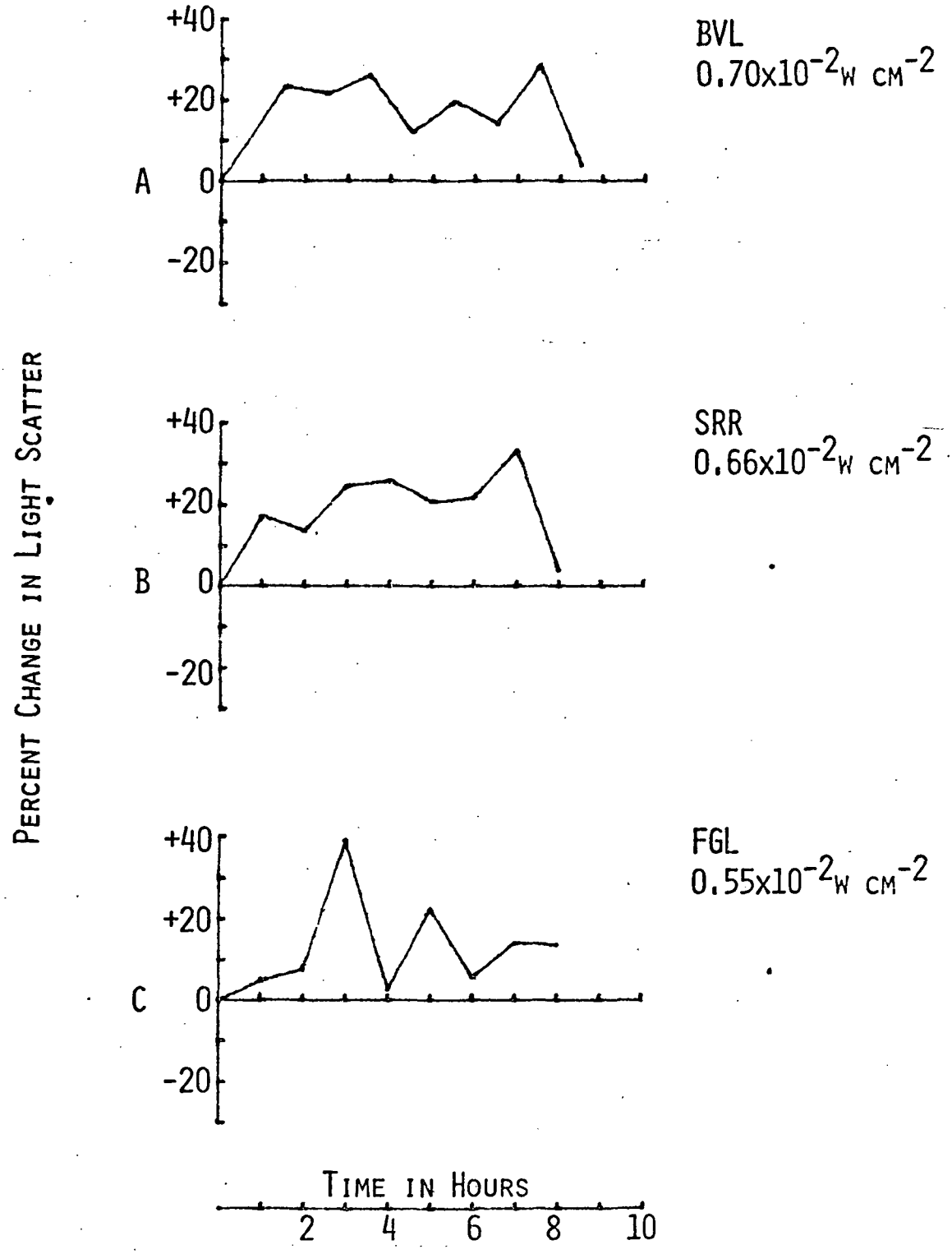

FIGURE 14. CORNEAL LIGHT SCATTER MEASUREMENTS FOR WAVEBAND 300 NM. SUBJECT CODE AND RADIANT EXPOSURE ARE INDICATED BY EACH GRAPH. THE SINGLE POINT TO THE RIGHT OF THE GRAPH INDICATES THE PERCENT CHANGE IN SCATTER 24 HOURS POST EXPOSURE.

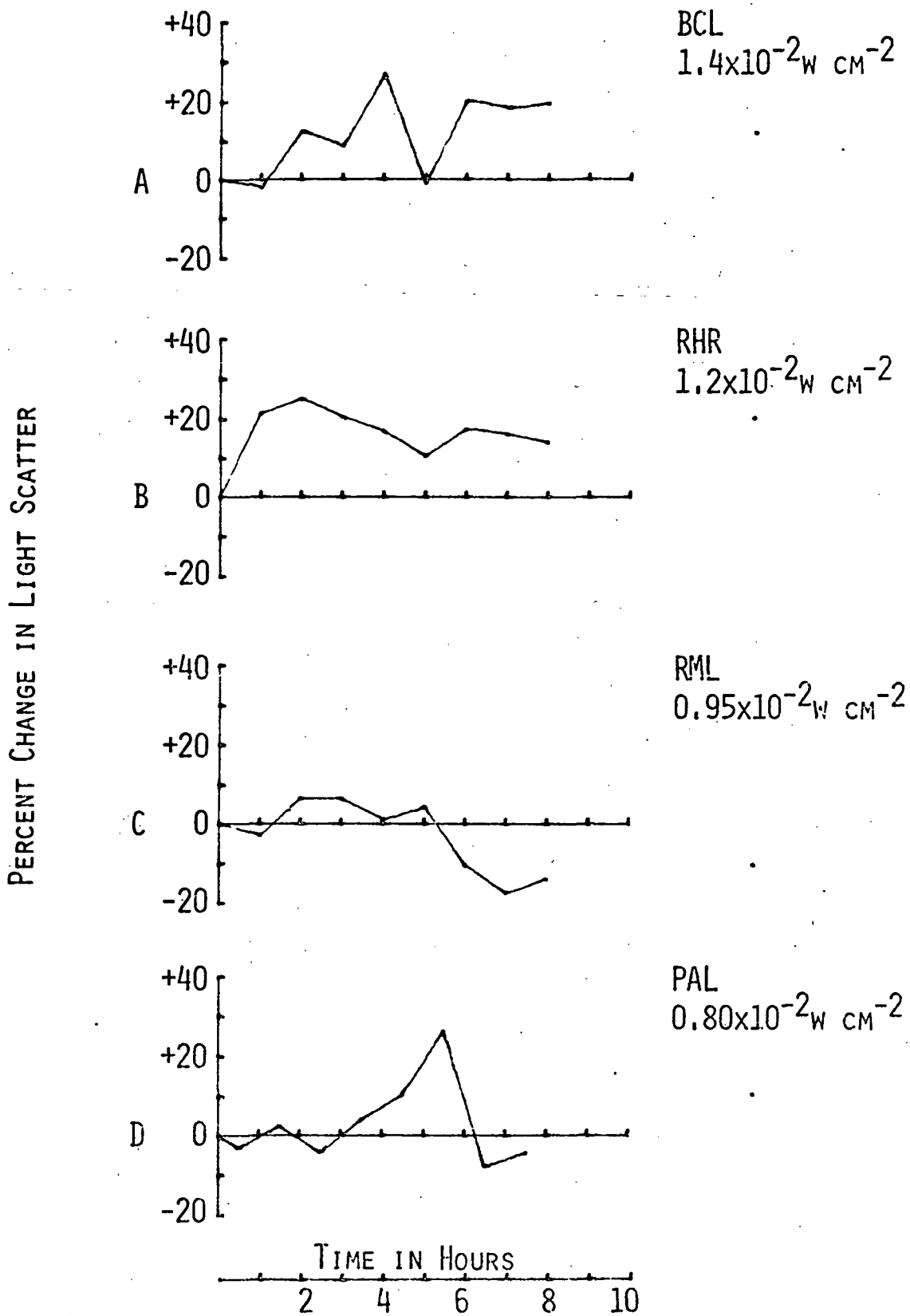

FIGURE 15. CORNEAL LIGHT SCATTER MEASUREMENTS FOR WAVEBAND 310 NM. SUBJECT CODE AND RADIANT EXPOSURE ARE INDICATED BY EACH GRAPH. THE SINGLE POINT TO THE RIGHT OF THE GRAPH INDICATES THE PERCENT CHANGE IN SCATTER 24 HOURS POST EXPOSURE.

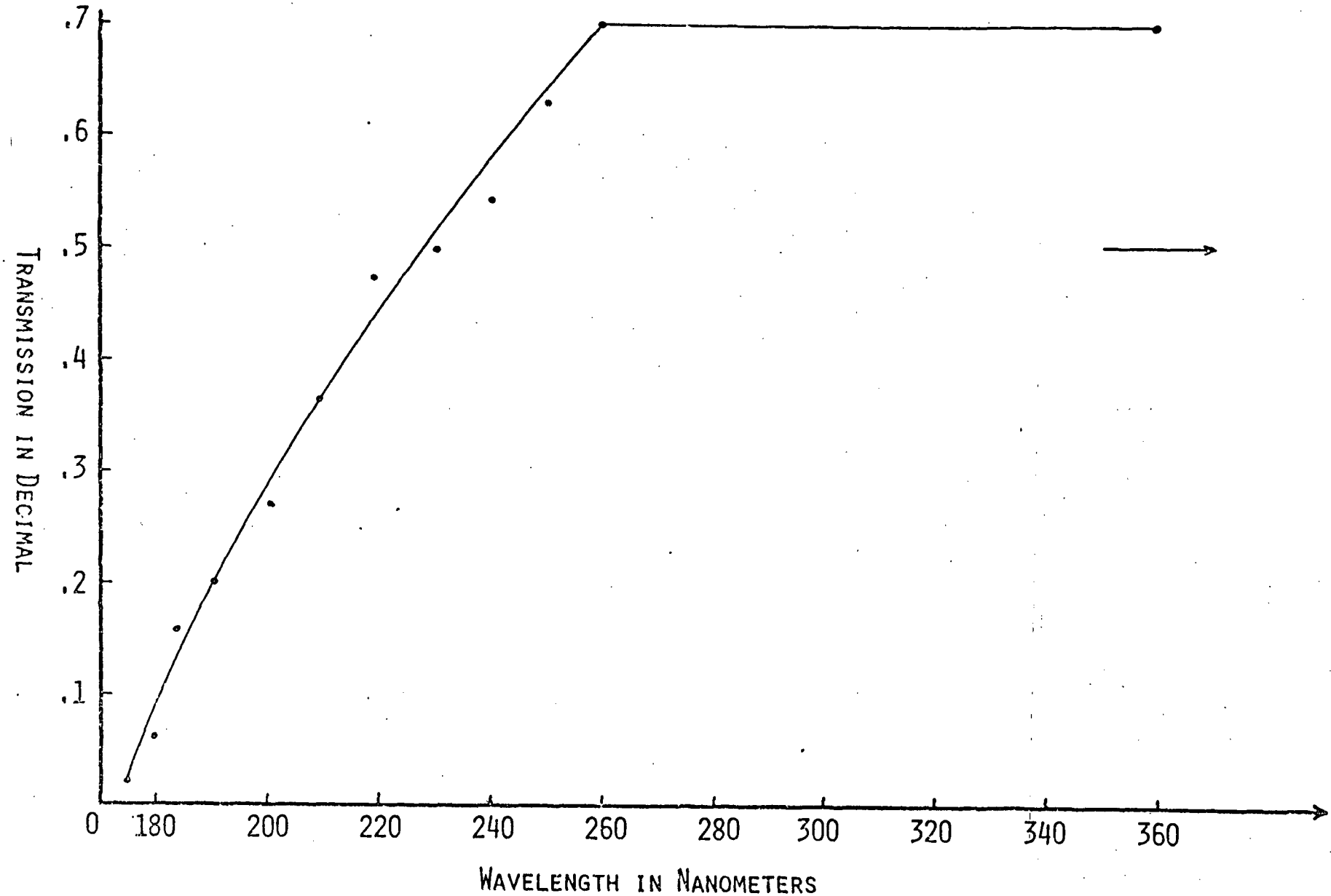

FIGURE 16. SOLAR TRANSMISSION THROUGH APOLLO R.H. UV GRADE WINDOW (3)

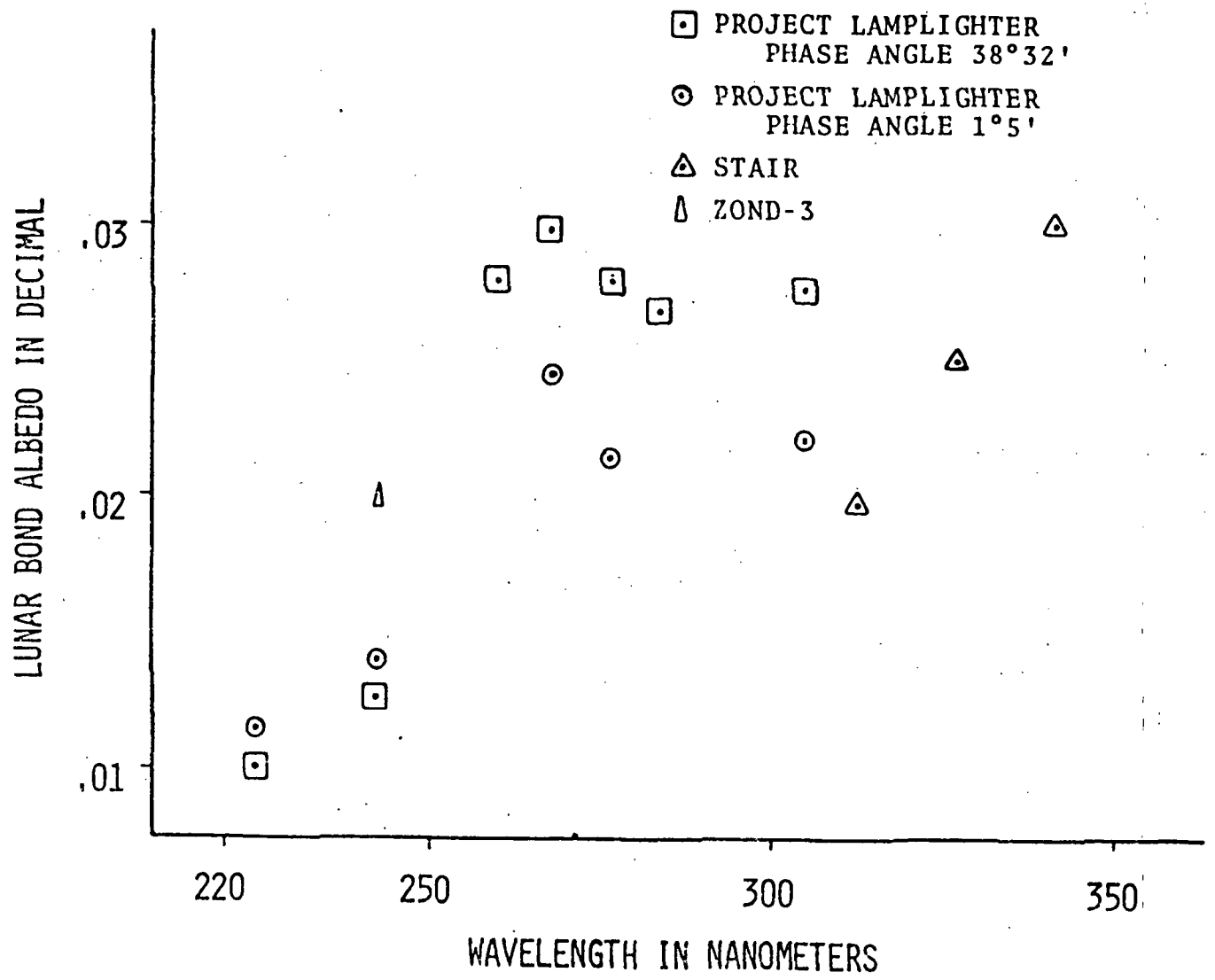

FIGURE 17. SPECTRAL REFLECTANCE OF SOLAR ULTRAVIOLET FROM THE SURFACE OF THE MOON

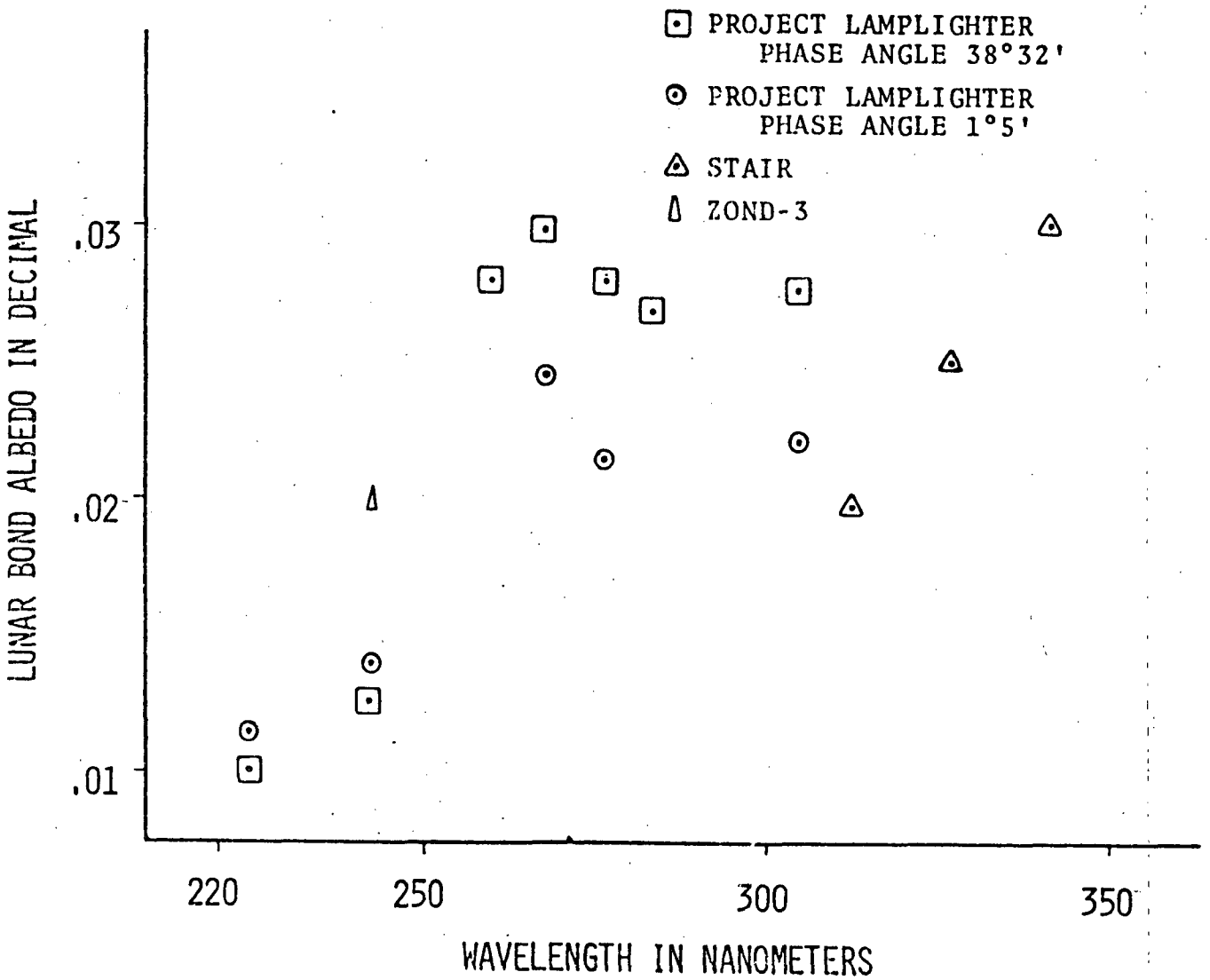

FIGURE 17. SPECTRAL REFLECTANCE OF SOLAR ULTRAVIOLET FROM THE SURFACE OF THE MOON